department of civil engineering
university of idaho
moscow, idaho
engineering experiment station

FINAL REPORT

An Investigation of the Transverse Distribution of Live Loads on a Post-tensioned Concrete Spread Box-girder Type Bridge

Donald F. Haber
David E. Rice
June 1972

Prepared For:
Idaho Dept. of Highways
and
Federal Highway Administration

Project Designation:
UI: 45-305
IDH: R-58

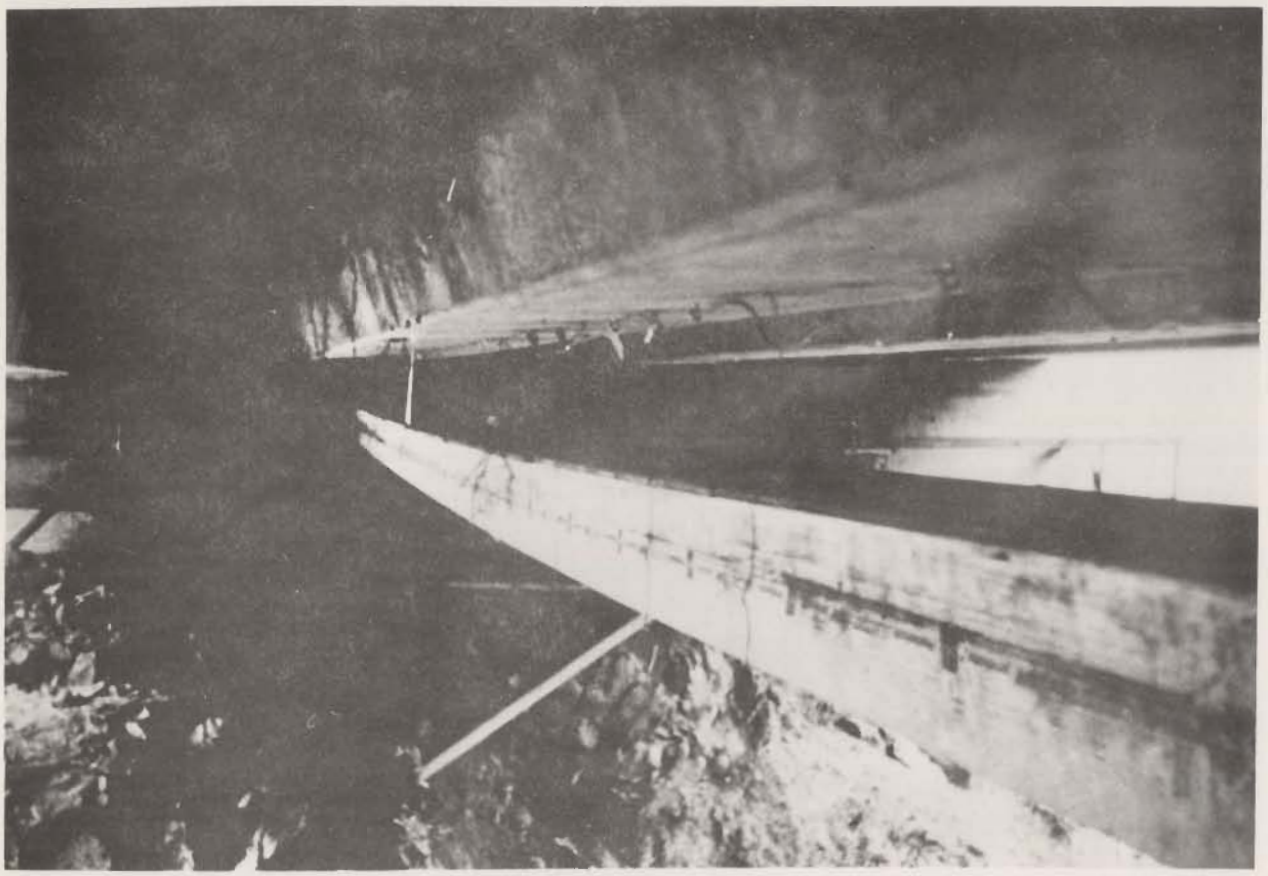

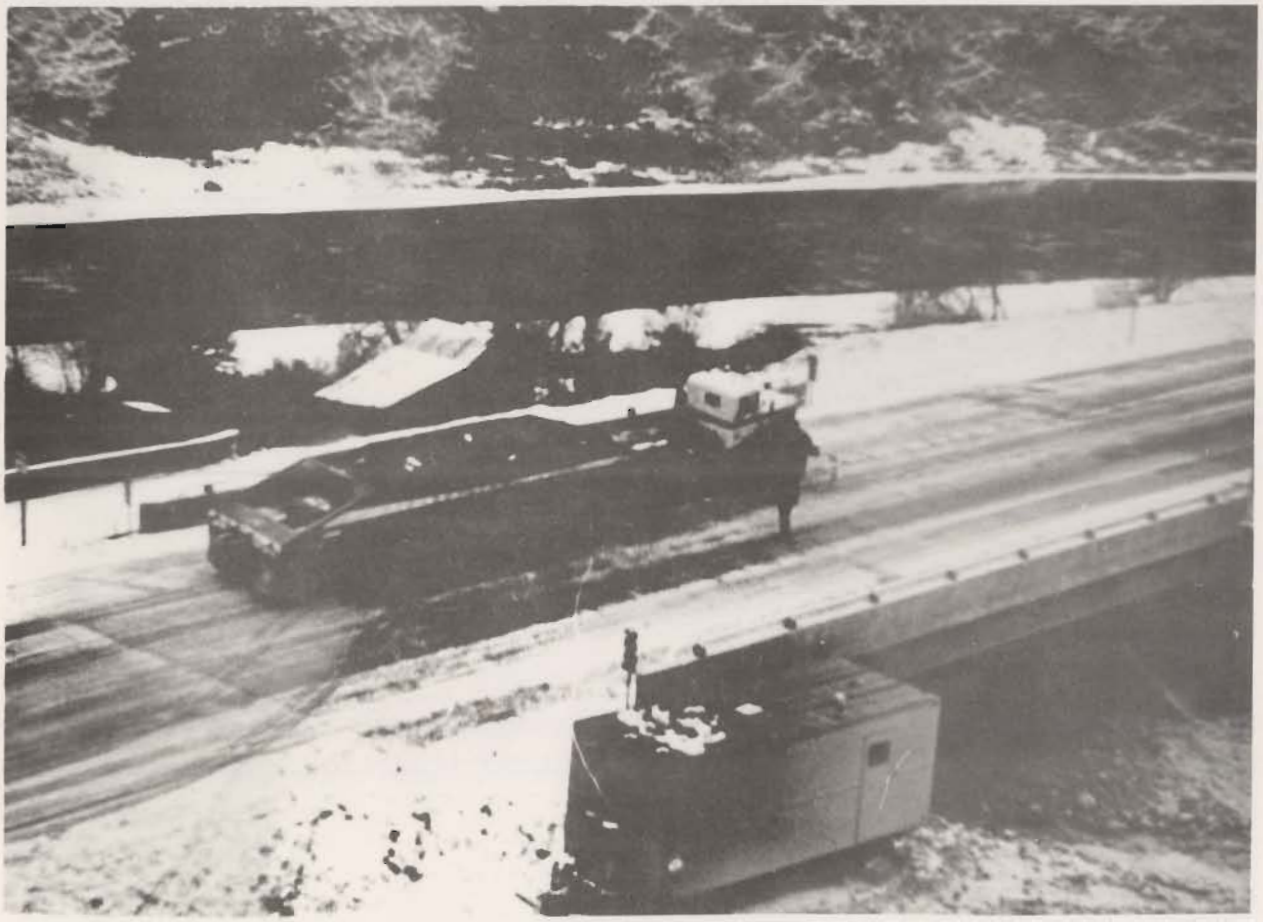

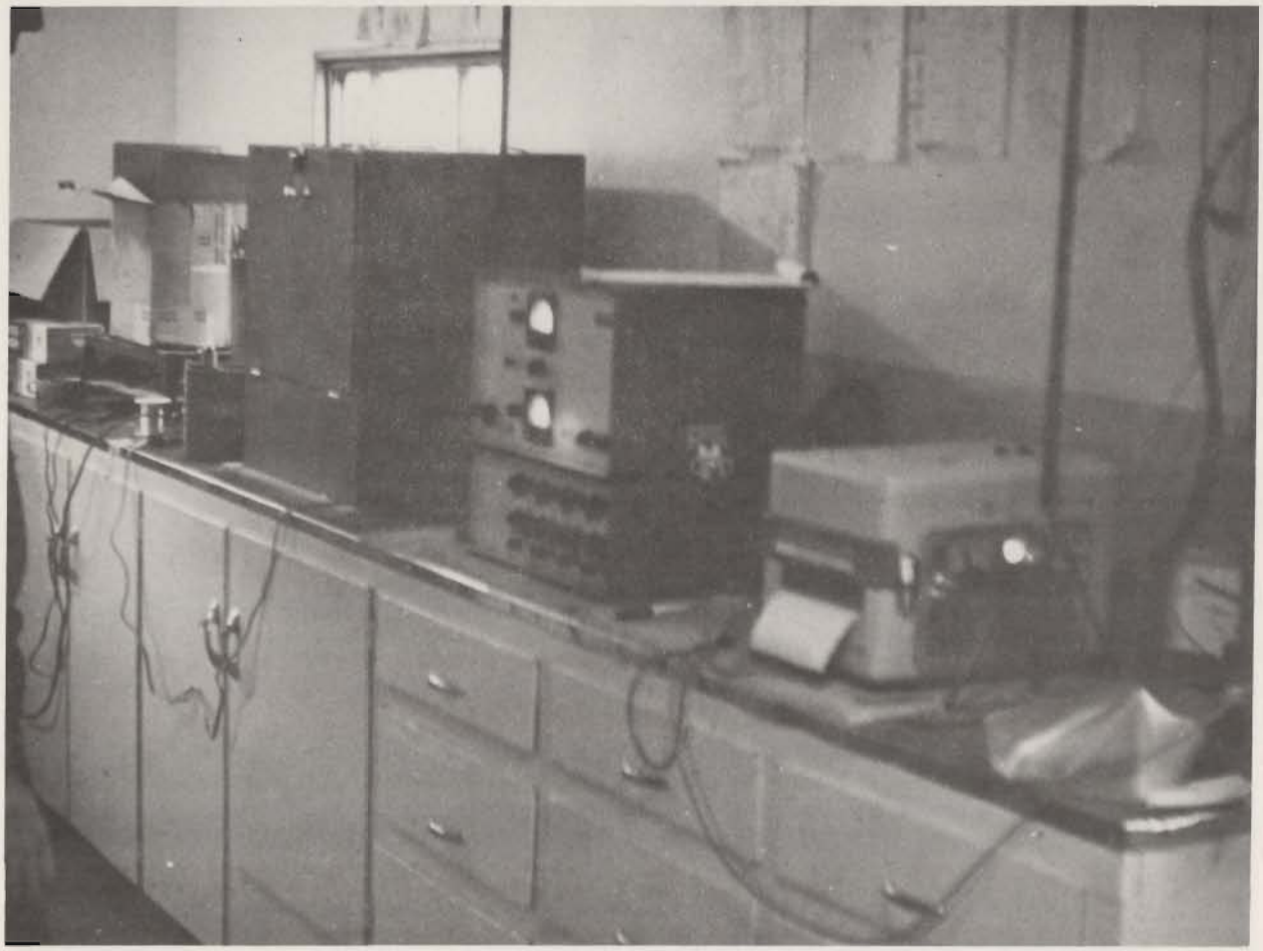

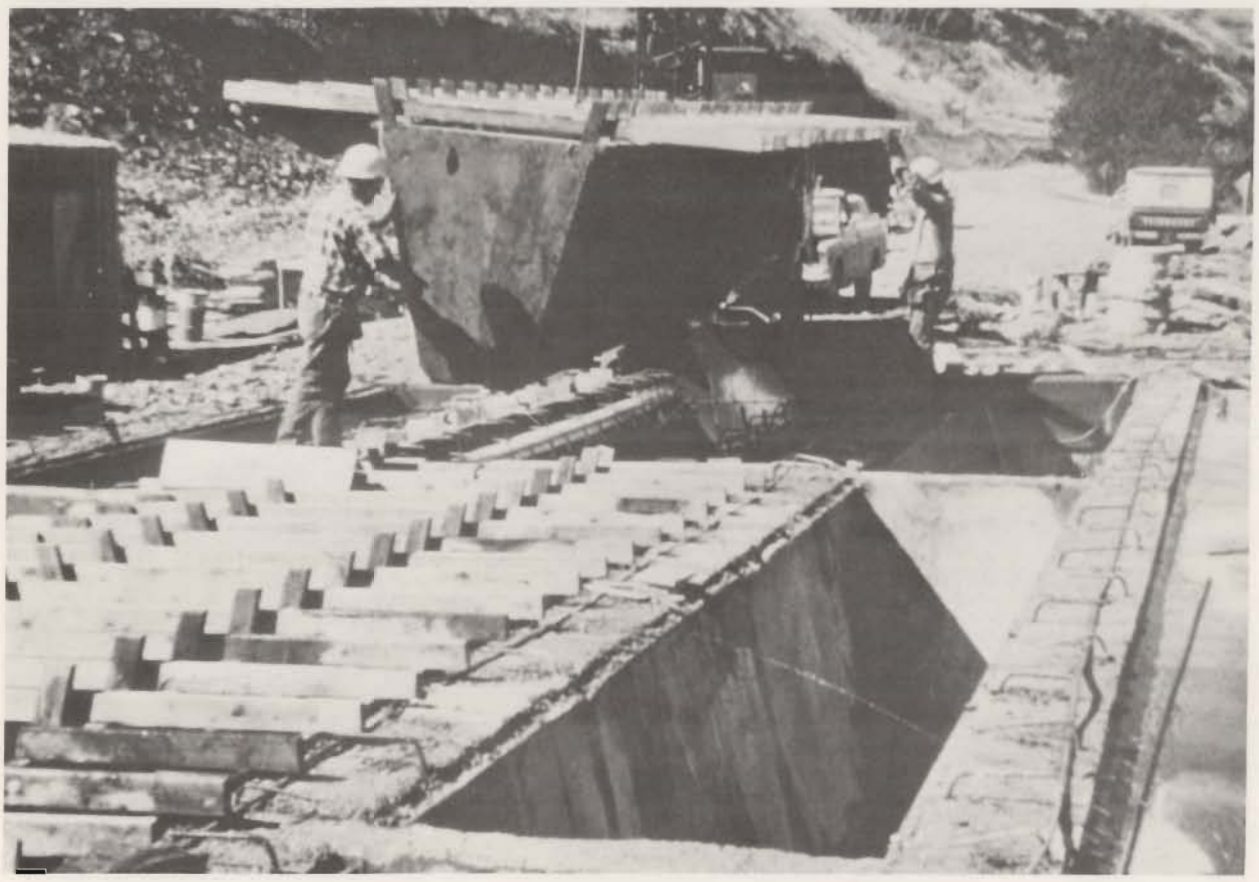

DEPARTMENT OF CIVIL ENGINEERING
UNIVERSITY OF IDAHO, MOSCOW, IDAHO 83843
RESEARCH PROJECT R-58 (45-305 U. of I.)

FINAL REPORT

AN INVESTIGATION OF THE TRANSVERSE DISTRIBUTION OF LIVE LOADS ON A POST-TENSIONED CONCRETE SPREAD BOX-GIRDER TYPE BRIDGE

by

Donald F. Haber

David E. Rice

Sponsored by

Idaho Department of Highways

and prepared in cooperation with the
U. S. Department of Transportation;
Federal Highway Administration.

June 1972

The contents of this report reflect the views of the author who is responsible for the facts and the accuracy of the data presented herein. The contents do not necessarily reflect the official views or policies of the State or Federal Highway Administration. This report does not constitute a standard, specification, or regulation.

TABLE OF CONTENTS

LIST OF TABLES

LIST OF FIGURES

ABSTRACT

The overall purpose of this investigation was to determine the experimental transverse live load distribution on a spread box-girder type bridge and to compare the results with similar studies of other bridges of this general type.

The test structure is a newly constructed bridge located near the mouth of Skookumchuck Creek in the Salmon River Canyon approximately four miles south of White Bird, Idaho. It consists of five cast-in-place and post-tensioned trapezoidal box girders, a composite cast-in-place reinforced concrete slab and reinforced concrete curbs. All of the tests were conducted with one series of gages. The bridge midspan was selected as the gage section for determination of the transverse live load distribution. In addition to the midspan section, gages were located along the longitudinal centerlines of the bottom surfaces of the girders to determine the location of the maximum bottom fiber strains. One gage was also embedded in the concrete approximately 1 1/2 inches from the bottom of each girder at its midspan. The wheel loads were induced by two test vehicles which were loaded with gravel to approximate the H 20-44 and HS 20-44 design trucks as specified in the AASHO Specification. The test runs were from north to south at 2 to 3 mph. Static strain responses were also taken and compared to the crawl run strain responses. The data in this report is based on the crawl run strain responses. Strain and deflection measurements were recorded by continuous strain recording equipment which was temporarily housed in a mobile trailer located adjacent to the bridge.

The field test data was reduced to strains and deflections. From the strain data experimental neutral axis location, moment percentage distributions, moment distribution coefficients, distribution factors and effective values of elastic moduli were determined. The moment percentages, ratios of experimental moments to design moments, distribution factors and bottom girder fiber strains were compared with similar quantities developed in the tests of the Drehersville, Berwick, White Haven and Philadelphia Bridges.

1. INTRODUCTION

1.1 Background

Since the first use of prestressed concrete beams in bridge construction, an increasing variety of beam cross sections have been proposed for bridge design. The development of new construction techniques both for prestressed and post-tension concrete beams has made these proposed designs a reality. The first common type of prestressed concrete beam was the I-beam type. These beams were usually incorporated in the bridge superstructure through shear connectors so that a portion of the deck was considered to be a part of the beam. Another common type of prestressed concrete beam was the T-beam where the top flange formed the deck. The procedure for the design of prestressed I-beam and T-beam concrete bridges are outlined in Section 1.3.1 of the AASHO Specifications for Highway Bridges.[1]

Prestressed box shaped beams were used in bridge construction first, by placing these beams side by side with a shear connector used to insure composite action, then a cast-in-place-reinforced concrete slab was constructed to act compositely with the beams. The next innovation was the spread box girder. The prestressed box beams were placed in a configuration similar to the I-beam configuration. The design of these spread box beam bridges also closely followed the AASHO Specifications. The cross section of the spread box beams are generally considered to be rectangular. However, trapezoidal box beams may offer advantages for the distribution of vehicular wheel loads. The results of a large amount of research on the load distribution of bridge floor systems has recently been correlated and summarized by W. W. Sanders, and H. A. Elleby of

Iowa State University.[2] In their report, Sanders and Elleby proposed a revision of the AASHO Specifications concerning the distribution of wheel loads for various types of bridge floor systems, including the spread box girder type.

The Bridge Section of the Surveys and Plans Division of the Idaho Department of Highways proposed a unique bridge design and it was constructed over Skookumchuck Creek on U. S. Highway No. 95 approximately four miles south of White Bird, Idaho. This design called for a seventy-foot simple-span prestressed concrete bridge with folded plate type prestressed concrete trapezoidal shaped box-girders, or simply U-shaped girders. The structural design was in accordance with the 1969 AASHO and 1970 Interim Specifications for Steel I-Beam stringers and prestressed concrete girders supporting a concrete deck.[2] This means each interior girder was designed to carry a certain percentage of the front and rear wheel loads. This percentage is called a distribution factor and for this design it was S/5.5, where S is the average girder spacing in feet. Once the slab is cast, however, the entire cross section will develop a greater torsional resistance than the I-beam bridge, and the transverse distribution of live load will be more efficient, than that for I-beam bridges. The spacings between interior girders could then be increased beyond what is allowed for I-beam stringers in Article 1.3.1 b (1) of the 1969 AASHO and 1970 Interim Specifications (S/5.5) and could approach or even exceed the distribution factor allowed for closed box-girders which have a distribution factor of S/7.0.[1]

This research project was undertaken to obtain field data and a theoretical analysis of a bridge supported by trapezoidal concrete spread box girders. The results of this research could then be used to add

reliability to the proposed new AASHO Specifications or could provide a basis for another proposal for AASHO wheel load distribution specifically applied to U-shaped concrete spread box-girder bridges.

1.2 Previous Research

1.2.1 Theoretical Research

Computer programs using three general methods for the analysis of box-girder bridges have been developed by Scordelis.[3] They are the Folded Plate Method, the Finite Segment Method and the Finite Element Method. The Folded Plate Method described by Scordelis[4] is based on the elasticity theory and utilizes plane stress elasticity theory and classical two-way thin plate bending theory to determine membrane stresses and slab moments in each plate. The Finite Segment Method is based on the ordinary theory for folded plates and uses a segment progression method along the span to connect one transverse segment to another until the far end of the bridge is reached.[3] The Finite Element Method is based on satisfying as closely as possible the assumptions for the elasticity theory for folded plates.[3] This method uses a numerical procedure to approximate the solution of a problem in continuum mechanics by analyzing the structure as an assemblage of finite elements interconnected at a finite number of nodal points. Selected internal stresses or displacement patterns are assumed in the elements to satisfy certain required conditions, usually nodal point compatibility and equilibrium.

A fourth general method of analysis of box-girder bridge structures is orthotropic plate theory. This method replaces the actual structure with an equivalent orthogonally anistropic plate that has the same transverse and longitudinal elastic and material properties as the actual

structure. This method has been limited in use because there has been some doubt as to what effective width should be used in replacing curb and parapet sections that would effectively allow for their stiffening effect. J. G. Arendts[5] developed a procedure for computing longitudinal and transverse flexural and torsional rigidities of three types of beam and slab systems; steel beams and concrete deck, non-voided concrete beams and separated box-girder concrete beams. He found that using these parameters in conjunction with orthotropic plate theory led to relatively simple calculations that adequately predicted the behavior of the three types of beam and slab bridge systems studied. Mr. Arendts also concluded that the present AASHO load distribution procedure results were not consistent with experimental results.

1.2.2 Field Test Research

Most of the field test investigations of highway bridges have been conducted on beam and slab bridges.[2] In 1964, the Structural Concrete Division of the Fritz Engineering Laboratory, Department of Civil Engineering at Lehigh University initiated a research project to investigate the actual structural behavior of bridges of the rectangular spread box-girder type and to develop a design procedure which would reflect their actual behavior.[10] The project involved spread box girders of rectangular cross section and related analytical studies of each[6,7,8,9]. In all of the test structures the experimental values of load distribution factors for interior girders were significantly less than those used for design, while the experimental values for the exterior girders were somewhat larger than those used for design. This behavior clearly emphasized the fact that the curb and parapet sections definitely and significantly contributed

to the longitudinal and flexural stiffness of the bridge superstructure.[10] From these studies it was recommended that consideration be given to revision of the procedures used for determination of the lateral distribution of vehicular loads for spread box-girder bridges. It was also recommended in the computation of deflection for design purposes, consideration be given to the inclusion of curb and parapet sections.

The actual field test data for these five bridges was obtained utilizing essentially the same technique. Trucks closely approximating the HS 20-44 design vehicle were driven over the test structure in a set of prescribed lanes. The response of the bridge was measured through the use of SR-4 electrical strain gages and recorded by continuous recording equipment. The strain gages were mounted around the periphery of the longitudinal beam at various cross sections on the surface of the beams.

Other tests of concrete box-girder bridges were conducted on bridges constructed by the California Department of Highways. These bridges were of the continuous box-girder type. The only reported field test to date was conducted on the Harrison Street Undercrossing in Oakland, California, by Davis, Kozak, and Scheffey.[11] The object of this test was to evaluate the validity of using distribution factors determined experimentally for this structure in the design of box girders with differing configurations and proportions. Assuming that analytical methods could be derived which would accurately describe the empirically determined structural behavior of the prototype, such analytical methods would then be applied to other structures. From the testing of this full-sized prototype it

was concluded that; (a) dead load deflections measured in the field agreed closely with those computed theoretically; (b) correlation of total dead load resisting moments with known acting moments is good provided that suitable modifications of the concrete modulus are made to account for effects of creep and shrinkage cracking; (c) live load distribution without an intermediate diaphragm indicated about 15 percent greater transverse distribution in the box girder than allowed in AASHO Specifications; (d) addition of a midspan diaphragm resulted in a very small change in the distribution of moments across the transverse section; and addition of curbs and parapets resulted in a large increase of total section stiffness.

1.3 AASHO CODE

Design of interior girders for bridges, for distribution of live load is presently based on distribution factors which represent the fraction of the total wheel load (both front and rear) carried by each girder. For spread box-girder bridges current design procedures use a distribution factor of S/5.5, where S is the average girder spacing in feet. This is the distribution factor for steel I-beam stringers and prestressed concrete girders supporting a concrete slab as prescribed in the 1969 AASHO Specifications 15, Section 3 - Distribution of Loads.[1] The distribution of live load for the exterior girders is based on the assumption that the slab acts as a simple beam between girders in transmitting wheel loads laterally. This specific part of the AASHO Specification is believed to be overly conservative.

2. THEORETICAL ANALYSIS

2.1 Folded Plate Analysis

The Folded Plate Method of analysis developed in a general computer program by A. C. Scordelis[3] is ideally suited to analyze box-girder bridges that are simply supported at both ends. The applied forces on the structure are first resolved into Fourier series components and an analysis is carried out for all of the loading components of each particular harmonic. The final results are obtained by summing the results for all of the harmonics. The basic assumptions of this method are:

1. Each plate of the box-girder bridge is rectangular, of uniform thickness and is made of an elastic isotropic and homogeneous material.

2. The relation between forces and deformation is linear so that superposition is valid.

3. The structure is completely monolithic.

4. End support and intermediate transverse diaphragms are infinitely stiff in their own plane, but perfectly flexible normal to their own plane.

5. The structure is simply supported at its extreme ends.

6. The stresses and displacements in each plate element due to loads normal to the plate (slab action) are determined by means of the classical thin plate bending theory applied to plates supported along all four edges.

7. The stresses and displacements of each plate element due to loads in the plane of the plate (membrane action) are determined by means of the elasticity equations that define the plane stress problem.

The structure is treated as a series of rectangular plates that are interconnected along their longitudinal joints. Each plate is first analyzed independently by two-dimensional plane stress theory for loads in the plane of the plate and by elastic plate theory for loads normal to the plane of the plate. The stiffness matrix for each plate is then expressed

in terms of the harmonics of a Fourier series. For each harmonic the plate has only four degrees of freedom along each longitudinal edge. These four degrees of freedom are: vertical and horizontal displacements in a plane parallel to the end diaphragms, a longitudinal displacement parallel to the joint and a rotation about an axis parallel to the joint. Then a direct stiffness solution is used to analyze the total structure consisting of the interconnected plates. Compatibility at the interior rigid diaphrams or supports is accomplished by a force (flexibility) method of analysis. The force method of analysis is similar in concept to that used to analyze a continuous beam. The redundant forces X represent a set of three joint forces at each longitudinal joint consisting of vertical, horizontal and rotational components in the plane of a transverse diaphragm at the one-third and two-thirds points across the transverse width of the plate. Since a rigid transverse diaphragm is assumed to exist at the interior support the displacements and rotations in the plane of the diaphragm of all points on this cross section of the bridge should be zero under the influence of the external loads and redundant forces. The Goldberg-Leve equations are used to evaluate plate fixed edge forces, stiffnesses and final internal forces, moments and displacements. A more detailed discussion of the method can be found in reference 3. For the support conditions mentioned the folded plate method permits an "exact solution" within the assumptions of the elasticity theory and for this reason may be used as a standard of comparison for other methods that are more general and based on simplifying but reasonable assumptions.

The general computer program for folded plate analysis, MUPDI[4], was

written in Fortran V language for the IBM 7094 computer at the University of California Computer Center, Berkeley, under the direction of A. C. Scordelis. A copy of the extended version of MUPDI, adapted to find girder moment percentages and run on the CDC 6400, was obtained and adapted to run on the IBM 360 model 67 computer at the Washington State University Computer Center.

2.2 Finite Element Analysis

The finite element method has been used successfully during the last ten to fifteen years to solve a large variety of problems such as plates subject to in-plane or normal loadings, axi-symmetric solids and axi-symmetric shells. More recently the finite element method has been applied to thin shell problems and three dimensional analysis of solids. A computer program FINPLA[12] has been developed by A. C. Scordelis which utilizes the finite element method for the analysis of prismatic cellular folded plate structures such as the box-girder bridge. The basic structural element, or finite element, is formed by dividing each rectangular plate transversely and londitudinally into an assemblage of smaller rectangular elements. The size, thickness and material properties of these rectangular elements can be varied as desired throughout the structure allowing for a finer mesh wherever more accuracy may be desired such as in zones near concentrated loads. It is assumed that each nodal point has six degrees of freedom for each of which exist a known external force or a known displacement. If a certain force is known the corresponding displacement is unknown and vice versa. A direct stiffness solution is used to find all of the unknown nodal point displacements and forces. Then the internal forces and stresses for each element can be determined. The crucial step

in this approach is the development of individual element stiffness matrices which can accurately approximate the behavior of the continuum when they are assembled to form the structure stiffness matrix needed in the direct stiffness solution.

The basic assumptions used in the finite element method are:

1. Each finite element is rectangular, of uniform thickness and is made of an elastic, isotropic and homogeneous material.

2. The relation between forces and deformations is linear so that superposition is valid.

3. The in-plane displacements within each rectangular finite element (membrane action) are obtained by the superposition of twelve displacement components at each corner of the element: two in-plane translations and one rotation about a normal to the plane of the element.

4. In-plane stresses within each finite element are determined from the in-plane displacements by means of the elasticity equations defining the plane stress problem.

5. The normal displacements within each rectangular finite element (slab action) are obtained by the superposition of twelve displacement patterns. These patterns are defined by three nodal point displacement components which are taken as two rotations about in-plane axes and a displacement normal to the plane of the plate.

6. The plate bending and torsional moments within each finite element are determined from the normal displacements by means of classical thin plate bending theory.

The assumptions (4) and (6) above are those of the elasticity theory for folded plates. It should be remembered that the complete structure assembled from the finite elements only approximates the true continuum since equilibrium and compatibility are satisfied only at the nodal points and not along the entire interfaces of adjacent elements. However, the independent displacement patterns chosen for the individual elements are selected to approximately satisfy compatibility across these interfaces. Once the element stiffness matrices have been derived by the Unit-displacement

theorem a direct stiffness solution may be used to solve the problem. A more detailed description of the derivation of the element stiffness solution is given in references 3 and 12.

The general computer program FINPLA[3] was written in Fortran IV language for the IBM 7094 computer at the University of California Computer Center, Berkeley, by A. C. Scordelis and C. Meyer. A copy of FINPLA was reproduced as reported in reference 3 and was adapted to run on the IBM 360 model 67 computer at the Washington State University Computer Center.

2.3 Test Bridge

Skookumchuck Creek Bridge is a seventy-foot simple-span post-tensioned spread concrete box-girder type bridge as shown in Figure 1. It has a skew of 15° from a line perpendicular to the longitudinal centerline and a superelevation of 6.35 per cent. The most unique characteristic of the bridge is its U-shaped girders that are shown in Figure 2.

2.4 Structure Idealization

The structure was idealized transversely and longitudinally in order to analyze it by using the computer programs MUPDI and FINPLA. The longitudinal or plan view was idealized as being rectangular. In a report by G. H. Powell, J. G. Bouwkamp and I. G. Buckle[13] it was shown that for varying angles of skew, from 0 to 20 degrees the sum of moments in all girders under varying loading conditions essentially remained unchanged. It was also noted, that the percentage of the total moment carried by an individual girder changed only slightly (less than 4%) as the skew varied from 0 to 20 degrees. The curbs on the bridge were idealized as longitudinal beams and were included in the finite element analysis. No post-tension stresses were included in the theoretical

analysis since only the live load strains were obtained from the experimental data.

2.5 Loading Lanes

Three different transverse loading lanes were used as loading conditions for the theoretical analysis of the structure using the finite element method of analysis. The three loading lanes consisted of the truck centerline located over the centerline of the bridge and two extreme loading lanes with the outside wheel of the vehicle two feet from the inside edge of either curb respectively. These three loading lanes were chosen since they closely represented the AASHO design condition used in connection with distribution factors. The results of each of the three loading lanes could then be superimposed and used for a theoretical distribution factor in comparison with the design and experimental distribution factors. The experimental loading lanes (1 through 5) are shown in Figure 3. Experimental loading lanes 1, 3 and 5 are the loading lanes in the finite element analysis. Since adapting the computer program FINPLA to run on the Washington State University computer was costly we were limited to the number of times that the program could be run. Once the global structure stiffness matrix is formulated any number of loading conditions can be imposed and solved without a significant increase in time or cost. The actual number of loading conditions that would be imposed on one particular idealized structure was limited by the maximum number of nodal points and finite elements allowed in a transverse cross-section.

The computer program MUPDI was used as a check on the computer program FINPLA since the results of MUPDI are considered to be exact for

an idealized structure and the results from FINPLA are approximations. MUDPI could not be used for the entire theoretical analysis due to limitations on the maximum number of nodal points and elements in a transverse cross section, and it does not have the added capability of including beam elements in the analysis. To compare FINPLA with MUDPI a Standard HS 20-44 truck with a modified axle width (an axle width compatible with the nodal point spacing on the structure) was symmetrically located on the bridge cross section and longitudinally placed for the maximum theoretical moment. This loading lane is shown in Figure 3 as loading lane 3.

2.6 Wheel loadings

Two sets of wheel loads and axle spacings that closely approximated those of the two test vehicles were used in each of the three lane loadings for the finite element analysis. The true wheel loads and axle spacings were input directly into the computer program. A weighted axle width based on the wheel loads was computed for each test vehicle. The average of the two weighted axle widths (which differed by less than one inch) was used as the axle width for the finite element analysis. The axle width on the HS 20-44 truck, which was used as the comparative loading condition, had to be restricted to the distance between the two nodal points at the junction of girder C and the slab. The wheel loads used for the comparative analysis are those specified by the AASHO Specifications for a standard HS 20-44 truck.

3. TESTING

3.1 Test Bridge

The test bridge is located on U.S. Highway 95 in the Salmon River

Canyon approximately four miles south of White Bird, Idaho. A picture of the bridge taken just after the approach slabs were poured is shown in Figure 4. The structure has a simply supported length of 70 feet and a skew of 15^{o} from a line perpendicular to the bridge centerline.

The cross section of the bridge as shown in Figure 2 consists of 5 identical cast-in-place post-tensioned hollow U-shaped box-girders, covered with a cast-in-place reinforced concrete deck. The U-shaped box-girders, which are 60 inches deep and taper from a width of 52 inches at the top to 30 inches at the bottom, are equally spaced at 8 feet, center to center. Diaphragms between girders were omitted in the design. The end diaphragms are 14 inches thick and the 6.5 inch deck provides a roadway of 39 feet 8 inches. The curb section consists of a tapered parapet section and a metal rail. The parapet is 18 inches wide at the bottom and tapers to 9 inches wide at the top at a height of 28.5 inches. The metal rail is a 4.5 inch outside diameter aluminum tube. The joint between the slab and the curb is a construction joint with a raked finish. Vertical reinforcement for the curb section extends through the joint into the slab.

The girders were designed for an HS 20-44 loading. A distribution factor of S/5.5 = 1.454 was used for the interior girders, while a distribution factor of We/7 was used for the exterior girders, where We is the top slab width as measured from the midpoint between girders to the outside edge. The distribution factors for girders A and E are 1.138 and 1.114 respectively. The design wind velocity is 80 mph and the impact factor is 0.258. The specified minimum 28-day cylinder strengths of the girder and deck concretes are 5000 and 3000 psi. respectively.

Each of the girders were post-tensioned with four 1.25 inch and one 1.375 inch diameter steel bars.

3.2 Gage Sections and Locations

The midspan of the bridge was selected for the gage section. Figure 5 shows the strain gage locations at midspan. Five gages were placed on each of the girders with the exception of girder C which had a total of eight gages. There were two gages located on the bottom edges of each girder and three located on the west side of each girder. Girder C had three gages located on its east side in addition to the three gages on the west side. All of the gages located on the sides of the girders were spaced at approximately one, two and three feet from the bottom of the girder. The deck has a total of nine gages three of which were located on the top of the deck at the bridge midspan (one was located at the centerline and the two others were placed next to the curb sections). The other six deck gages were located on the underside of the deck at midspan at the midpoint between girders and on the east and west edges of the deck. The two curb sections were gaged at the bridge midspan at the top and bottom of their outside faces. Each of the five girders had one gage embedded in the center of the bottom flange at the bridge midspan. Only four of these gages were operable during the tests because the lead wires for the embedded gage in girder A were pulled out when the falsework was removed from the underside of the bridge. A total of sixteen gages were located longitudinally along the centerlines of the girders. Girders A, B, D, and E, each had three gages along their centerlines located at three, six and nine feet north of midspan. Girder C had four gages located along its centerline at three, six, nine and twelve feet north of midspan. These gages were used to determine the position

of maximum live load strains. In a report by Robert F. Varney[14] it was noted that the maximum observed strain responses for interior girders of skew bridges did not occur at the theoretical maximum moment section calculated for a simple beam loading. Mr. Varney also noted that the maximum bending moment stress in the exterior girders occurred at or near midspan for all test vehicle crossings on all paths. Deflectometer responses were recorded for the center of each girder for all the loading lanes.

3.3 Loading Lanes

Three of the loading lanes were located such that the centerline of the truck would correspond with the centerline of the bridge and the centerlines of the north bound and south bound traffic lanes. The two other loading lanes were such that the outside wheels of each vehicle would be located two feet from the inside edge of either curb. The five loading lanes are shown in Figure 3.

3.4 Test Vehicles

Two test vehicles were used for the testing phase. A photograh of the first test vehicle, a three axle diesel dump truck, and the axle spacings and axle loads are shown in Figure 6. The second test vehicle was a three axle diesel tractor semi-trailer combination, with the axle loads and axle spacings as shown in Figure 7. Both vehicles were loaded with gravel.

3.5 Instrumentation

Basically, four different types of strain gages were used to record the strain. Most of the gages were a special type of encapsulated gage

distributed by Anderson-Lowery Associates and designeted as PLM-60. These gages were mounted on the girder and deck surfaces, however, five of the gages were embedded directly in the concrete during construction approximately 1 1/2 inches from the bottom of the girders. The PML-60 gages had a gage length of 60 mm, a gage resistance of 120 $\pm$ 0.5 ohms and a gage factor of 2.13. Two paper backed gages (PL-120) were used to provide comparison with the PML-60. The two paper backed gages were mounted adjacent to two of the PML-60 gages at midspan on girder C. These gages had a gage length of 100 mm, a resistance of 120 $\pm$ .03 ohms and a gage factor of 2.06. The third type of gages used was an encapsulated gage (PML-100S). The PML-100S gages had a gage length of 100 mm, a resistance of 300$\pm$ .0 ohms and a gage factor of 2.11. The PML-100S gages were mounted on girders C, D, E and are shown in Figure 5 as dotted lines. A photograph of a PML-6- strain gage mounted on a girder face is shown in Figure 8.

Three tapered cantilevered aluminum beams were manufactured such as the one shown in Figure 10 and were used to record deflections. The beams were 1/8 inch thick and tapered from 1 inch to 4 3/8 inches over a 12 inch length. Each beam was instrumented with four strain gages at the wide end to measure flexural strains. The gages used were SR-4 Type A3 wire resistance strain gages. The wide end of the beam was bolted to the bottom surface of the girders by using inserts that were placed in girders during construction. The apex of the plate was connected to a weight on the ground surface below the deflectometer by a wire. The wire was adjusted to introduce an initial deflection in the aluminum plate. Each deflector was calibrated beforehand so that a change in flexural strain, occurring when the bridge deflected could be converted to deflections.

The recording equipment consisted of a Honeywell Model 119 Carrier and Linear/Integrate Amplifier and a Honeywell Model 906C Visicorder Oscillograph. The amplifier consisted of a power supply and four amplifiers capable of receiving and amplifying input from four active gages simultaneously. The amplified signals were then recorded on light sensitive paper by the oscillograph. Sheathed cable was used to transmit the signals to the amplifiers. Four active gages were recorded at a time. Dummy gages were used for temperature compensation. The same lengths of sheathed cable that were connected to the active gages were connected to the dummy gages to allow for the change in inductance of a signal transmitted through a long cable. Once the dummy gages were hooked up it was only necessary to change active gages through the use of cannon plugs. During the testing the recording equipment was housed in a mobile trailer provided by the Idaho Department of Highways. The position of the test vehicles was noted by the use of voice signals.

3.6 Test Runs

A total of 326 individual test runs were made by the two load vehicles. These test runs included; the crawl test runs at 2 to 3 mph; static load tests where the vehicle came to a complete stop over a prescribed location on the bridge; and several dynamic test runs at speeds between 35 and 50 mph. Since only four recording channels were available for each test run, the test vehicles had to cycle through all lane loadingsbefore a new set of four gages could be activated. This procedure was repeated until all the strain gages had been activated and the strains recorded.

The calibration procedure was to shunt a known value of resistance

did not plot in a linear fashion with the other strains along the cross-section were discarded, although nearly all of the strains did plot in a linear fashion. Since the anomaly did not appear on both tests, the most probable reason for the variation of some strain measurement points from the linear when plotted at a cross section was due to extreme wind gusts at certain times on the exposed wire leads.

At those strain gage locations where the strain cross-section plots for both test vehicles did indicate an anomaly (two locations) from the linear, it was felt the gages were improperly placed rather than the structure acting non-compositely giving the anomalous results. Typical locations for neutral axes for interior and exterior girders are shown in Figure 9.

4.2 Evaluation of Girder Moment Percentages and Effective Values of Elastic Modulus

A computer program was written to calculate girder moment percentages and effective values of elastic modulus. Two methods of calculating girder moment percentages and values of elastic moduli were used. Input for the program included, experimental location of the neutral axes, the tensile and compressive girder strains, the compressive deck and curb strains, the strains on the transformed post tension steel areas, the maximum bottom fiber strains and the value of the theoretical maximum moment.

4.2.1 Calculations Using a Center-to-Center Girder Spacing

The first method assumed a center-to-center spacing for the effective slab width for all the girders. It calculated a ratio of the deck elastic modulus to the girder elastic modulus, for each girder, based on the ratio

of the first moments of the transformed tensile and compressive areas. This balanced the compressive and tensile forces. The forces and moments on the section calculated by transforming the post-tension steel were added into the results obtained by integrating the concrete strains over the cross section. For the loading conditions used it was felt that the live load strain in the post-tension steel was approximately the same as the live load strain in the concrete surrounding the post-tension duct at the midspan. In order for this assumption to be valid the live load moment within the vicinity of the bridge midspan has to be symmetrical. Although the live load moments within the vicinity of the bridge midspan are not symmetrical they are nearly so. The post-tension bars were also grouted and it was felt this added to the validity of the assumption. The results for all the loads by this method agreed very well with the second method of moment percentage calculation. Then the internal moments were equated to the known external moments to determine the absolute values of the effective deck and girder elastic moduli, based on the experimental location of the neutral axis. Last the percentages of the total moment carried by each girder was calculated.

4.2.2 Calculations Using Effective Slab Widths

The second method used for the calculation of girder moment percentages and effective values of elastic modulus involved the use of effective slab widths and only one value of elastic modulus for the curb, deck and girders. The amount of slab width required to balance the first moment of the tensile area and the first moment of the compressive area was the effective slab width. The effective slab widths of the exterior girders were modified by one of two methods depending on the slab width of the

adjacent interior girder. If the effective slab width of the adjacent interior girder was greater than the center-to-center spacing of the girders only the portion of the slab remaining above the exterior girder was considered to be contributing to the exterior girder cross-section. If the effective slab width of the adjacent interior girder was less than the center-to-center spacing of the girders, the contributing slab width of the exterior girder was considered to be the center-to-center spacing of the girders.

Next, the principal axes were located for each effective girder cross section and the moments of inertia about the principal axes were calculated. Moment coefficients were then calculated based on the maximum bottom fiber strains and the moments of inertia about the principal axes. Moment coefficients are the moments divided by the elastic modulus. The effective values of elastic modulus were calculated by equating the internal moment to the known external moment. Last, the percentages of the total moment carried by each girder were calculated.

In all of the calculations full composite action was assumed between the girders, slab and curbs. The distribution of live load moment as calculated by the two methods differs by less than two percent and values of effective elastic moduli in both cases are in good agreement.

4.3 Distribution Factors

In the AASHO Specifications[1] provisions for lateral distribution of live load in bridges are expressed as distribution factors. These factors are coefficients by which a line of wheel loads is multiplied in computing the design moment for a girder. The AASHO Specifications also specify that for the design of girders the centerline of a wheel

or a wheel group shall be assumed to be at least 24 inches from the face of a curb. Moreover, the Specifications state that the loads, or standard trucks, shall be assumed to be occupying any position within their individual design traffic lane which will produce the maximum stress. In order to make the experimental load distribution comparable with the AASHO provisions, distribution percentages with a test truck in various lanes were superimposed to approximate the specified design loading. The roadway width of the bridge between curbs is 36 feet 9 3/16 inches and was designed for three traffic lanes each having a width of 12 feet 3 1/16 inches. Therefore a close approximation of the AASHO design loading was produced when the trucks were located in loading lanes 1, 3 and 5. The experimental distribution factor for a girder was obtained by summing the girder moment percentages for that girder with the truck in lanes 1, 3 and 5 and multiplying by two since distribution factors are given in terms of wheel loads rather than axle loads.

5. TEST RESULTS

5.1 Moment Percentages and Neutral Axes

The moment percentages for the girders are shown in Table 1 and Figures 11 - 14. Each of the moment percentages shown represents the percentage of total moment carried by the particular girder for the designated load lane. The results for both trucks are shown. The girder moment percentages presented in Table 1 are based on calculations that assume a center-to-center spacing for effective slab widths, the experimental location of the neutral axis and different values of elastic modulus for the slab and girders. The curbs were assumed to have

the same elastic modulus as the deck. Figures 15 and 16 show the resulting moment percentages for loading lanes 1, 3 and 5 superimposed for the dump truck and tractor trailer respectively. Figures 17 and 18 show the resulting moment percentages for loading lanes 2 and 4 superimposed for the dump truck and tractor trailer respectively. Influence lines for the moment percentages for each of the girders are shown in Figures 19 - 23. (Actually, these are not influence lines in the strict sense of the definition, but are the moment percentages carried by one particular girder with the trucks in various loading lanes.) Experimental locations of neutral axes are shown in Figure 24.

5.2 Distribution Coefficients

Distribution coefficients which are defined as the percentage of the total moment coefficient carried by each girder are shown in Table 2. A moment coefficient is defined as the moment divided by the modulus of elasticity. The distribution coefficients are based on calculations that equated the internal and external forces by using an effective slab width for each girder. The calculations also assume the same value of effective elastic modulus for the curbs, slab and girders.

5.3 Distribution Factors

The distribution factors were determined as explained in Section 4.3. The experimental and design distribution factors and their ratios for each of the girders are shown in Table 3. The results for both test vehicles are listed.

5.4 Experimental Live Load Moments and Effective Values of Elastic Modulus

The experimental live load moments and effective values of elastic

modulus for each girder are listed in Table 4. The results are based on calculations that assumed a center-to-center spacing for effective slab width, the experimental location of the neutral axes and different values of elastic modulus for the slab and girders. The curbs were assumed to have the same elastic modulus as the slab.

5.5 Moment Coefficients and Effective Values of Elastic Modulus

The moment coefficients and corresponding values of elastic modulus for each of the girders are listed in Table 5. A moment coefficient is the moment divided by the elastic modulus. The values in Table 5 are based on calculations that used effective slab widths, maximum bottom fiber strains and moments of inertia about the principal axes for each girder.

5.6 Effective Slab Widths

The effective slab widths as used in the second method of moment percentage calculation are listed in Table 6. They are calculated as described in Section 4.2.2. The effective width of 96.00 inches which often appears in the table is the maximum slab width available for the exterior girders. The effective slab width of 77.00 inches which also appears in the table is the minimum slab width available for the exterior girders.

5.7 Girder Deflections

Midspan girder deflections for each loading lane and test vehicle are listed in Table 7 and shown in Figure 25. All of the deflections listed are deflections of the girder centerline.

5.8 Response of Embedded Gages

A comparison of the strains recorded by the embedded gages and the two bottom surface gages for girders B, C, D and E are listed in Table 8. The responses for girder A are not listed because the gage embedded in girder A was inoperable.

5.9 Maximum Bottom Fiber Strain

The theoretical maximum moment locations for the dump truck and the tractor trailer are 0.62 feet north and 5.14 feet south of midspan respectively, with both trucks facing south. Because of a limit on the number of gages, it was decided to try and locate the maximum bottom fiber strains caused by the dump truck only. For that reason the sections north of midspan were gaged as described in Section 3.2. In order to record the responses of the PML-100S gages, which had resistances of 300 ohms, it was necessary to replace the two internal 120 ohm resistors in each amplifier with two 300 ohm resistors in order to complete the wheatstone bridge circuit. Nearly all of the responses of the PML-100S gages had to be discarded because they were erratic and inconsistent. This was probably caused by the questionable quality of the 300 ohm resistors in the amplifiers. However, the responses of the PML-60 gages located longitudinally along the bottom centerlines of girders A and B were felt to be reliable, and are shown in Table 9.

6. DISCUSSION OF RESULTS

6.1 Theoretical Results

The results of the transverse live load distributions for the comparative analyses between MUPDI and FINPLA are in good agreement as shown in Figure 28. Figures 29 and 30 show the transverse and longitudinal variations of the deflections of the bridge under the comparative loading condition. The effect of the curb sections, idealized as longitudinal beams, in the finite element analysis is quite evident. The absolute values of total maximum moment at midspan as calculated by the two programs differ by about 10 percent. The discrepancy is due mainly to some of the assumptions inherent in the finite element analysis such as equilibrium and compatibility being satisfied at the nodal joints only. A computer program was written to calculate the total moment at a section and the girder moment percentages from the output of FINPLA which consisted of average nodal point stresses per unit length and average nodal point moments per unit length. The stress distribution between nodal joints was assumed to be linear and the average element forces were integrated over the entire cross section.

The results of the final finite element analysis are in very good agreement with the experimental results. The theoretical and experimental distributions of moment percentage differed by less than 2 percent. The experimental and theoretical midspan girder deflections are in very close agreement when the experimentally determined effective

values of elastic modulus are taken into consideration. The values of the theoretical moment for each girder obtained from the superposition of the loads in loading lanes 1, 3 and 5 for both trucks agreed reasonably close to the similar values obtained experimentally. Table 14 shows the moment percentage distribution for the two test vehicles as caluculated by the finite element theory and corresponding ratios of the theoretical and design distribution factors. Table 10 lists the moment percentages from the finite element analysis and the ratios of the theoretical and design distribution factors.

6.2 Moment Percentages

Comparisons of moment percentages at the bridge centerline with either of the two test vehicles in different test lanes indicated results that would be expected for a spread box-girder structure. Girders nearest the load carried the larger portion of the load. The superelevation of the structure increased the distribution of moments to the girders on the low side of the superelevation. The effect is most noticeable in a comparison of the percentage of moment carried by girders A and E for a symmetrical load condition. Also the effect of superelevation can be shown by a comparison of the moment carried by girder A with the vehicle in loading lane 5 and the moment carried by girder E with the vehicle in loading lane 1. The effect of superimposing the results for loading lanes 1, 3 and 5 gives a nearly equal distribution to all five girders. Again the effect of superelevation slightly increases the moment percentage for girder A. Superimposing lanes 2 and 4 shows a nearly equal

distribution to all five girders and the superelevation is not very noticeable. The moment percentage distribution results from the two test vehicles differed by less than 2 percent as shown by the plots of the influence lines for the five girders in Figures 19 - 23. The effect of the axle loads of the dump truck being more localized than those of the tractor trailer can be noticed in a comparison of the moment percentage distributions as shown in Figures 11 and 13. The superelevation of the bridge is also evident in a comparison of the influence lines for beams A and E in Figures 19 and 23. The stiffening effect of the curbs on the exterior girders is apparent as shown in Figures 15 - 18.

6.3 Distribution Coefficients

The distribution coefficients as defined in Section 5.2 and shown in Table 2 are in very good agreement with the moment percentages although the two were determined by two different methods. The method used in calculating distribution coefficients has been used successfully in other investigations.

6.4 Distribution Factors

The distribution factors for the two test vehicles were in very good agreement. The experimental distribution factors are 1.395 and 1.387 for girder A and 1.239 and 1.226 for girder E. These correspond to the AASHO design distribution factors of 1.138 and 1.114 for girders A and E respectively. For interior girders the experimental distribution factors range between 1.067 and 1.206, or in the form presented in the AASHO Specification, $S/7.50$ and $S/6.63$. The ratios of the experimental distribution factors to the design distribution factors for the exterior girders are all greater than one, ranging between 1.225 and 1.101 while

the ratios for the interior girders are all less than one, ranging between 0.734 and 0.829.

A comparison of the ratios of experimental distribution factor to design factor for the Drehersville, Berwick, White Haven, Philadelphia and Skookumchuck Creek bridges is listed in Table 10. The ratios for the exterior girders of Skookumchuck Creek Bridge agree fairly well with those for the Berwick, White Haven and Philadelphia Bridges ranging from 1.083 to 1.228 while those for the Drehersville Bridge are 1.404 and 1.389. The ratios for the interior girders for the Drehersville, Berwick, White Haven and Philadelphia Bridges are in very close agreement ranging from 0.601 to 0.657 while the ratio for Skookumchuck Creek Bridge is 0.774. The difference may be attributed to beam cross sections since Skookumchuck Creek has trapezoidal shaped girders rather than rectangular box-girders as the other bridges. The design of Skookumchuck Creek Bridge also incorporated the top flange of the girders into the deck while the decks on the other bridges were cast essentially on the top of the girder flanges. In all of the structures the box beams and the slab were considered to act as a composite section. The interior girder live load distribution for Skookumchuck Creek Bridge is in the range between the AASHO Specifications and the results for the previously mentioned rectangular box-girder bridges. The distribution of live load to the exterior girders for Skookumchuck Creek Bridge is greater than the AASHO design factor would indicate and agrees with the live load distributions for the other bridges mentioned.

6.5 Live Load Moments and Moment Coefficients

The live load moments at the bridge centerline are shown in Table 4 and are in the range expected. The live load moments were determined as

explained in Section 4.2.1. The moment coefficients as defined in Section 4.2.2 are listed in Table 5. The moment coefficients when multiplied by the proper values of elastic modulus are in good agreement with the live load moments.

6.6 Comparison of Design Experimental and Theoretical Live Load Moments

The ratios of the experimental moments over the design moments for each girder for the two test vehicles are listed in Table 11. Both exterior girders have ratios greater than one ranging from 1.100 to 1.224 while the interior girders have ratios less than one ranging between 0.750 and 0.830. Figures 26 and 27 show a comparison of the design, theoretical and experimental moments carried by each girder caused by superimposing the results for the test vehicles in loading lanes 1, 3 and 5. The experimental and theoretical moments for the exterior girders are greater than the corresponding design moments while the experimental and theoretical moments for the interior girders are less than their corresponding design moment. A comparison of the ratios of the experimental moments to the design moments for the Drehersville, Berwick, White Haven, Philadelphia and Skookumchuck Creek Bridges is listed in Table 12. The interior girder ratios for Skookumchuck Creek Bridge are all greater than the corresponding ratios for the other bridges while the exterior girder ratios for Skookumchuck Creek Bridge closely agree with the same ratios listed for the Berwick, White Haven and Philadelphia Bridges.

6.7 Effective Values of Elastic Modulus

The effective values of elastic modulus that were determined by using a center-to-center girder spacing as explained in Section 4.2.1

are listed in Table 4. The values for the curbs and deck are less than the values for the girders. The values of elastic modulus that were determined by using effective slab widths as explained in Section 4.2.2 are listed in Table 5. These values fall in between the values listed in Table 4. All of the values are greater than those that have been reported previously[9,10,11]. A comparison of the maximum strains on the bottom surfaces of the girders for the White Haven, Berwick and Skookumchuck Creek Bridges is shown in Table 13. In general, the experimental values of effective elastic modulus do not agree well with the results from cylinder tests and design calculations based on the density and the compressive stress fc'. Other investigations[11] also have not been able to draw a correlation between the design and effective values of elastic modulus. The values of the effective elastic modulus are substantially higher than those used normally in design. The design value is a function of fc', the 28 day compressive strength of the concrete. The value of fc' after the structure is in use is usually significantly greater than the 28 day value used in design. It is very common for beam concrete to reach the specified 28 day cylinder strength at, or shortly after, release of the pre-tensioning elements.

The elastic modulus based on a test cylinder taken as the girder was poured gave design values of about $E = 5 \times 10^6$ psi., while a test of one of the cylinders using a PML-60 strain gage gave a modulus of $E = 7.5 \times 10^6$ psi. These tests were run four months after the girder was poured.

6.8 Strains, Neutral Axes and Effective Slab Widths

Plots of strain along the side faces of girders normally showed a linear relationship. The curb and deck strains plotted linearly with the girder strains indicating full composite action between the girder, deck and curbs. However, referring to Figure 5, it should be pointed out that there were four strain gages on the right side of girders A, B, D and E and only two gages on the left side, that is, one on the bottom of the girder and one on the bottom of the deck. The use of four strain gages on each girder face made any non-linearities readily apparent and added reliability to the linear results.

Assuming full composite action, the experimental locations of the neutral axes were nearly always inclined except when the loads were directly above the girder as shown in Figure 24. The inclinations were the greatest when the loads were farthest away from the girder. The neutral axes of the interior girders were horizontal when the loads were directly above the girder such as girder C and loading lane 3. Even though the exterior girders have an unsymmetrical cross section the neutral axes were very nearly horizontal when the loads were closest to them. Variations between the vertical locations of neutral axes with respect to the bottom girder faces also occurred. This distance was usually greater when the truck was laterally located nearer to the girder.

The effective slab widths as described in Section 4.2.2 are listed in Table 6. These values should be considered with some reservations since a small change in neutral axis location causes a relatively large variation in the effective slab width[7]. The value of the slab width for

a girder is generally greatest when the load is nearest that girder. The value of 96.00 inches which appears frequently for the exterior girders is the maximum slab width available for the exterior girders (based on a center-to-center spacing) and the value of 77.00 inches is the minimum slab width available above the girder.

6.9 Girder Deflections

The girder deflection, listed in Table 7 and illustrated in Figure 25, are of the expected magnitude. The values are generally about one-third of those reported for other spread box-girder bridges such as the Philadelphia and White Haven Bridges. The moment of inertia of Skookumchuck Creek Bridge is about three times the value of the moments of inertia of the Philadelphia and White Haven Bridges. The effect of superelevation on the girder deflections is very evident for symmetric loading conditions. A very good agreement between the experimental and theoretical girder deflections was found when the experimentally determined values of elastic moduli were used in the theoretical calculations.

6.10 Embedded Gages

The responses of the embedded gages shown in Table 8 are generally slightly greater than those of the externally mounted gages. The difference in most cases was less than 4 percent. Overall, the externally mounted gages performed just as well as the embedded gages and there is no benefit in embedding the gages in the structure as opposed to mounting them on the outside surface.

6.11 Maximum Bottom Fiber Strains

For reasons explained in Section 5.9, the data on the location of

maximum bottom fiber strains is limited. The results for girders A and B are shown in Table 9. The maximum bottom fiber strains for girder A, an exterior girder, occur at or near midspan regardless of the transverse location of the vehicular loads. The maximum observed strain responses for girder B, an interior girder, generally did not occur at the theoretical maximum moment section calculated for a simple span beam loading. However, the maximum strains on girder B do occur at sections closer to the theoretical maximum moment section as it carries more load.

7. CONCLUSIONS AND IMPLEMENTATION

The following conclusions were made based on the results of the field testing of Skookumchuck Creek Bridge.

1. The experimental distribution factor for the interior girders was less than the AASHO design distribution factor, but greater than the experimental distribution factors resulting from the testing of rectangular box-girder bridges. For the exterior girders the design distribution factor was less than the experimentally based value which agreed with the results from the rectangular box-girder bridges. The participation of the curbs in carrying load served to provide added stiffness and strength to the exterior girders. For interior girders the design factor of the S/5.5 form should be modified to yield lesser values. Based on these results and the close agreement between these results and the results of the field testing and analysis of rectangular box-girder bridges, it is recommended that consideration be given to change the design factor for the distribution of wheel loads. It is recommended that the design factors be S/6.0 for the interior girders and S/7.5 for the exterior girders for this size of bridge (five girders and two lanes).

   Furthermore, close consideration should also be given to the design change proposed by Sanders and Elleby[2] even though their proposed design is based on an analysis which precludes the effects of curbs and parapit sections (which results in the same design factor for both exterior and interior girders).

2. The strains recorded during the field testing all plotted linearly. The curb, deck and girder cross sections all responded compositely.

3. The strain gages mounted on the outside surface of the structure gave as reliable results as those that were embedded in the concrete.

4. The effective values of elastic modulus were determined by two procedures and the results from each corresponded quite well. The experimental values, however, are greater than the design values and reasons for this are given in Section 6.6. In general, the values of effective elastic modulus resulting from the field testing of bridges are greater than the design values based on the density and f_c'.

5. The superelevation of the bridge did affect both the moment percentage distribution to the girders and the girder deflections.

6. The theoretical results agreed closely with the experimental results in comparing the transverse live load distribution and the girder deflections. Based on this result, use of either of the two computer programs for strain and deflection data for other bridges of this type would be feasible. Load limitations for existing bridges of the beam and slab type could be easily determined given the modulus values and the stiffness parameter values.

7. Based on two theoretical analyses the curbs seem to have little effect on the transverse live load distribution, but they do affect the deflections of the structure. It would be desirable to include the effects of the curbs in the design deflection calculations.

8. Based on the comparison of the theoretical analysis, which assumed no skew, and the experimental results, the skew had no significant effect.

8. ACKNOWLEDGEMENTS

This study was conducted in the Department of Civil Engineering at the University of Idaho under the auspices of the Engineering Experiment Station, College of Engineering as a research investigation sponsored by the Idaho Department of Highways.

The field test equipment was made available through the Department of Civil Engineering at the University of Idaho.

Acknowledgement is gratefully made to the following people for their assistance in the field work and other services: Mr. Bob Jarvis, Senior Bridge Engineer, Mr. Leif Erickson, Materials and Research Engineer, Mr. Lee Hatch, Associate Research Engineer, Mr. Marvin Lotspeich, District Engineer, Mr. Kay Montgomery, Resident Engineer and Mr. Jim Ross, Engineer-in-Training.

Acknowledgement is also gratefully made to Mr. Richard Pape for tracing the figures and to Mrs. Jan McGraw and Miss Becky Rauch for typing the manuscript.

9. REFERENCES

1. American Association of State Highway Officials, STANDARD SPECIFICATIONS FOR HIGHWAY BRIDGES, Ninth Edition, AASHO, Washington, D.C. 1965.

2. Sanders, W. W. and Elleby, H.A., DISTRIBUTION OF WHEEL LOADS ON HIGHWAY BRIDGES, National Cooperative Highway Research Program Report 83, Highway Research Board, 1970.

3. Scordelis, A. C., ANALYSIS OF CONTINUOUS BOX GIRDER BRIDGES, Structures and Material Research Report No. SESM-67-25, University of California, (1967).

4. Scordelis, A. C., ANALYSIS OF SIMPLY SUPPORTED BOX GIRDER BRIDGES, Structures and Materials Research Report No. SESM-66-17, University of California, (1966).

5. Arendts, J. G., STUDY OF EXPERIMENTAL AND THEORETICAL LOAD DISTRIBUTION IN HIGHWAY BRIDGES, Unpublished M.S. Thesis, Iowa State University, (1968).

6. Douglas, W. J. and Van Horn, D. A., LATERAL DISTRIBUTION OF STATIC LOADS ON A PRESTRESSED CONCRETE BOX BEAM BRIDGE - DREHERSVILLE BRIDGE, Fritz Engineering Lab. Report 315.1, Lehigh University Institute of Research, (1966).

7. Guilford, A. A., and Van Horn, D. A., LATERAL DISTRIBUTION OF VEHICULAR LOADS IN A PRESTRESSED CONCRETE BOX BEAM BRIDGE - BERWICK BRIDGE, Fritz Engineering Lab. Report 315.4, Lehigh University Institute of Research, (1967).

8. Guilford, A. A., and Van Horn D. A., LATERAL DISTRIBUTION IN A PRESTRESSED CONCRETE BOX BEAM BRIDGE - WHITE HAVEN BRIDGE, Fritz Engineering Lab. Report 315.7, Lehigh University Institute of Research, (1968).

9. Lin, C. and Van Horn, D. A., THE EFFECT OF MIDSPAN DIAPHRAMS ON LOAD DISTRIBUTIONS IN A PRESTRESSED CONCRETE BOX BEAM BRIDGE - PHILADELPHIA BRIDGE, Fritz Engineering Lab. Report 315.6, Lehigh University Institute of Research, (1968).

10. Van Horn, D. A., STRUCTURAL BEHAVIOR CHARACTERISTIC OF PRESTRESSED CONCRETE BOX BEAM BRIDGES, Fritz Engineering Lab. Report 315.8, Lehigh University Institute of Research, (1969).

11. Davis, R. E., Kozak, J. J., and Scheffey, C. F., STRUCTURAL BEHAVIOR OF A CONCRETE BOX GIRDER BRIDGE, Highway Reserach Record No. 76, (1965), pg. 32-82.

12. Scordelis, A. C., COMPUTER PROGRAM FOR PRISMATIC FOLDED PLATES WITH PLATE AND BEAM ELEMENTS, Structure and Materials Research Report No. SESM 70-3, University of California, (1970).

13. Powell, G. H., Bouwkamp, J. G. and I. G. Buckle, BEHAVIOR OF SKEW HIGHWAY BRIDGES, Structures and Materials Research Report SESM 69-9, University of California, (1969).

14. Varney, R. F., PHASE 3 OF A PRELIMINARY RESEARCH REPORT ON AN EXPERIMENTAL LOADING STUDY OF THREE HIGHWAY BRIDGES IN TENNESSEE WITH THE U.S. ARMY HET-70 MAIN BATTLE TANK TRANSPORTER, Structures and Applied Mechanics Division, Office of Research and Development, Bureau of Public Roads, Washington, D. C., (1970).

10. TABLES

Table 1. Moment Percentages at the Bridge Midspan

$$\text{MOMENT PERCENTAGE} = \frac{\text{MOMENT}}{\Sigma\text{MOMENTS}} (100)$$

	DUMP TRUCK GIRDER					TRACTOR TRAILER GIRDER				
	A	B	C	D	E	A	B	C	D	E
Lane 1	5.46	5.73	13.05	31.73	44.04	5.01	6.71	14.42	30.02	43.84
Lane 2	6.30	8.06	18.42	34.67	32.35	6.88	8.25	19.00	31.46	34.41
Lane 3	13.92	20.15	34.84	17.65	13.43	15.15	20.76	32.65	18.65	12.78
Lane 4	35.66	33.37	16.45	7.79	6.74	35.87	32.37	16.80	8.90	6.06
Lane 5	50.40	27.47	11.17	6.51	4.46	49.18	27.07	13.24	5.86	4.66

(calculations are based on the experimental location of the neutral axis and a center-to-center spacing for the girder flanges)

Table 2. Distribution Coefficients at the Bridge Midspan

$$\text{DISTRIBUTION COEFFICIENT} = \frac{\text{MOMENT COEFFICIENT}}{\Sigma\text{MOMENT COEFFICIENTS}} (100)$$

	DUMP TRUCK GIRDER					TRACTOR TRAILER GIRDER				
	A	B	C	D	E	A	B	C	D	E
Lane 1	6.27	5.70	12.63	30.30	45.10	5.14	6.68	14.17	29.15	44.86
Lane 2	6.55	8.01	18.25	33.48	33.71	7.10	8.11	18.70	30.89	35.20
Lane 3	14.19	20.15	34.41	17.53	13.72	15.61	20.64	31.76	18.55	13.45
Lane 4	36.65	32.72	16.19	7.70	6.74	36.89	31.90	16.19	8.84	6.18
Lane 5	50.37	27.23	11.20	6.59	4.61	49.08	26.73	12.92	5.85	5.41

Table 3. Distribution Factors at the Bridge Midspan

(Calculations based on the experimental location of the neutral axis and a center-to-center spacing for the girder flanges)

	DUMP TRUCK			TRACTOR TRAILER		
	Experimental		Experimental / Design	Experimental		Experimental / Design
Girder A	1.395		1.225	1.387		1.218
Girder B	1.067	$\frac{S}{7.50}$	0.734	1.091	$\frac{S}{7.33}$	0.750
Girder C	1.181	$\frac{S}{6.77}$	0.812	1.206	$\frac{S}{6.63}$	0.829
Girder D	1.118	$\frac{S}{7.16}$	0.769	1.091	$\frac{S}{7.33}$	0.750
Girder E	1.239		1.112	1.226		1.101

AASHO DESIGN FACTORS: INTERIOR = 1.454
EXTERIOR, GIRDER A = 1.138 GIRDER E = 1.114

Table 4. Moments at the Bridge Midspan (lb-ft.)

(calculations are based on the experimental location of the neutral axis, and a center-to-center spacing for the girder flanges)

	DUMP TRUCK T.M. = 808,000 (lb-ft)* GIRDER					TRACTOR TRAILER T.M. = 790,000 (lb-ft)* GIRDER				
	A	B	C	D	E	A	B	C	D	E
Lane 1	44,077	46,266	105,445	256,351	355,861	39,566	52,991	113,891	237,187	346,366
Lane 2	52,498	65,133	148,794	280,150	261,424	54,367	65,138	150,069	248,550	271,876
Lane 3	112,474	162,848	281,524	142,645	108,509	119,672	164,026	257,972	147,358	100,972
Lane 4	288,105	269,623	132,883	62,942	54,448	283,375	255,760	132,737	70,279	47,849
Lane 5	407,224	221,958	90,244	52,575	35,999	388,493	213,858	104,579	46,292	36,778

MODULUS OF ELASTICITY (10^6 psi)

	GIRDER	DECK	GIRDER	DECK
Lane 1	8.47	7.39	9.13	7.69
Lane 2	8.64	6.79	8.80	6.95
Lane 3	8.42	6.44	9.17	7.83
Lane 4	8.72	6.30	9.55	7.43
Lane 5	8.46	5.78	9.67	7.06

*Theoretical Moment

Table 5. Moment Coefficients at the Bridge Midspan (10^{-6} ft-in^2)

(calculations are based on the location of the principal axes and the effective slab widths)

	DUMP TRUCK T.M. = 808,000 (lb-ft)* GIRDER					TRACTOR TRAILER T.M. = 790,000 (lb-ft)* GIRDER				
	A	B	C	D	E	A	B	C	D	E
Lane 1	6,802	6,181	13,706	32,874	48,930	5,002	6,503	13,791	28,372	43,669
Lane 2	6,902	8,451	19,246	35,307	35,548	7,202	8,226	18,966	31,338	35,711
Lane 3	15,205	21,596	36,870	18,784	14,705	14,965	19,788	30,448	17,782	12,894
Lane 4	38,612	34,464	17,059	8,107	7,102	34,661	29,972	15,214	8,304	5,802
Lane 5	54,617	29,527	12,141	7,140	5,002	45,814	24,953	12,055	5,464	5,052

	MODULUS OF ELASTICITY (10^6 psi)	
Lane 1	7.45	8.12
Lane 2	7.66	7.79
Lane 3	7.54	8.24
Lane 4	7.67	8.41
Lane 5	7.45	8.46

* Theoretical Moment

Table 6. Effective Slab Widths
(inches)

	DUMP TRUCK GIRDER					TRACTOR TRAILER GIRDER				
	A	B	C	D	E	A	B	C	D	E
Lane 1	96.00	54.21	67.65	127.62	77.00	96.00	72.86	92.06	108.41	77.00
Lane 2	96.00	62.60	72.87	123.34	77.00	96.00	82.96	82.19	79.25	96.00
Lane 3	96.00	78.24	88.52	78.61	96.00	96.00	68.05	152.21	68.56	96.00
Lane 4	96.00	87.56	74.34	64.15	96.00	96.00	82.76	155.40	77.27	96.00
Lane 5	96.00	87.31	56.56	54.98	96.00	96.00	87.77	92.50	41.17	96.00

Table 7. Girder Deflections (inches)

	DUMP TRUCK GIRDER					TRACTOR TRAILER GIRDER				
	A	B	C	D	E	A	B	C	D	E
Lane 1	0.00552	0.00875	0.01473	0.02528	0.02855	0.00421	0.00788	0.01525	0.02603	0.02999
Lane 2	0.00705	0.01093	0.01839	0.02600	0.02256	0.00551	0.01044	0.01907	0.02634	0.02428
Lane 3	0.01337	0.02243	0.02523	0.01783	0.01039	0.01225	0.02047	0.02399	0.01784	0.01182
Lane 4	0.02539	0.02885	0.01643	0.00841	0.00529	0.02611	0.02530	0.01598	0.00863	0.00610
Lane 5	0.03269	0.02610	0.01285	0.00655	0.00427	0.03167	0.02339	0.01288	0.00649	0.00475
Lanes 1, 3 & 5 (superimposed)	0.05158	0.05728	0.05281	0.04966	0.04321	0.04813	0.05174	0.05212	0.05036	0.04656
Lanes 2 & 4 (superimposed)	0.03244	0.03978	0.03482	0.03441	0.02785	0.03162	0.03574	0.03505	0.03497	0.03038

Table 8 . Comparison of Strains Recorded by Bottom Surface and Embedded Strain Gages. (10^{-6} in/in)

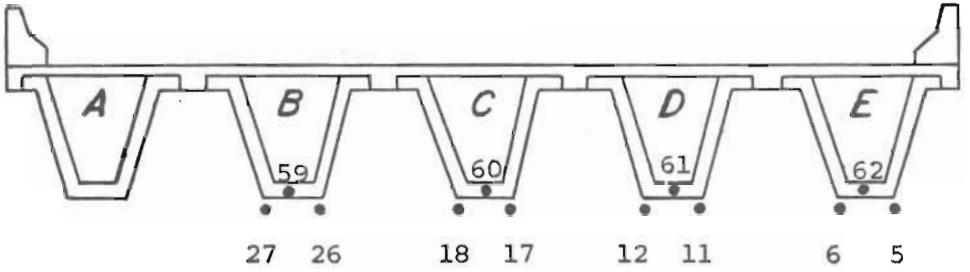

	27	59	26	18	60	17	12	61	11	6	62	5
						DUMP TRUCK						
Lane 1	4.35	4.59	3.91	9.12	9.53	8.24	20.69	20.64	20.93	22.05	25.89	23.87
2	5.59	5.87	5.00	12.71	12.98	11.30	24.50	23.17	21.22	16.38	18.46	16.20
3	13.25	14.54	13.02	24.15	23.32	21.84	12.60	12.43	12.04	7.02	7.67	7.29
4	21.53	23.72	21.93	11.44	11.56	11.05	5.23	5.68	6.02	3.00	3.60	3.24
5	20.08	20.40	17.37	8.05	8.72	8.48	4.04	4.21	5.45	2.00	3.12	2.83
						TRACTOR TRAILER						
Lane 1	4.66	3.90	3.17	9.37	8.86	8.34	17.20	19.03	13.60	20.73	19.98	20.97
2	5.49	5.63	4.87	12.05	12.24	11.14	20.23	19.25	20.39			
3	13.17	13.00	12.18	19.40	19.41	18.69	9.86	10.50	13.59			
4	19.20	19.08	18.51	9.37	9.92	9.09	4.55	5.47	6.52			
5	16.73	16.48	14.38	8.03	7.60	7.58	4.30	3.28	3.80	2.16	3.77	2.73

Table 9. Maximum Fiber Strains Caused by The Dump Truck for Girders A and B.

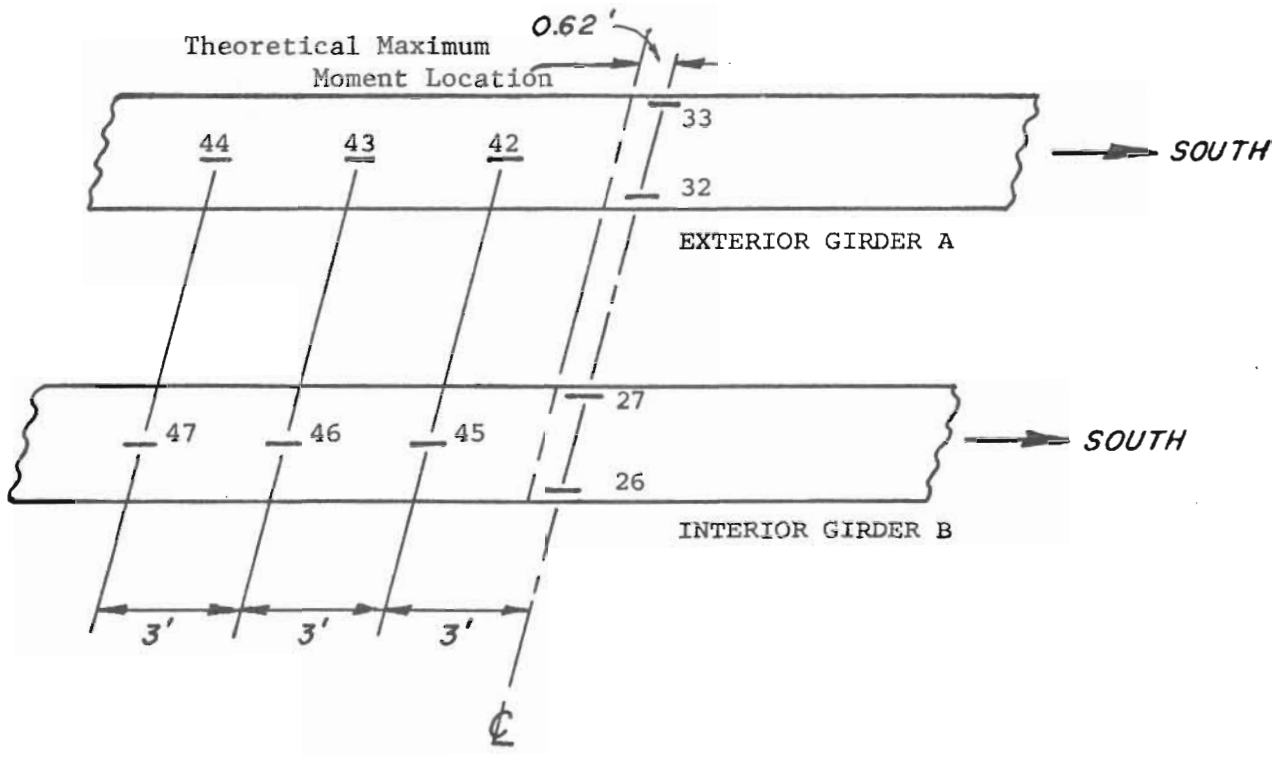

	GAGE NUMBER									
	26	27	45	46	47	32	33	42	43	44
Lane 1	3.91	4.35	2.93	5.79	6.02	3.22	3.38	2.97	2.21	2.12
Lane 2	4.99	5.59	4.20	8.91	10.53	3.22	3.59	3.56	2.88	2.59
Lane 3	13.03	13.25	13.19	21.39	18.56	7.08	7.60	6.82	6.63	5.41
Lane 4	21.93	21.53	17.98	30.75	20.56	19.59	18.57	17.21	13.93	11.05
Lane 5	17.37	20.08	31.77	26.74	18.56	26.31	26.38	23.74	20.57	12.69

Table 10. Summation of Distribution Factors for Drehersville, Berwick, White Haven Philadelphia and Skookumchuck Bridges.

Bridge	Direction	Experimental	Design	$\frac{\text{Experimental}}{\text{Design}}$	Moment of Inertia 10^6 in^4
		Exterior Girder			
Drehersville*	East	1.137	0.810	1.404	1.33
Drehersville*	West	1.125	0.810	1.389	
Berwick	North	1.178	1.050	1.122	1.58
Berwick	South	1.137	1.050	1.083	
White Haven	North	1.228	1.000	1.228	1.60
White Haven	South	1.212	1.000	1.212	
Philadelphia**		1.283	1.158	1.108	2.19
Skookumchuck	South	1.311	1.126	1.164	4.94
		Interior Girder			
Drehersville*	East	0.854	1.30	0.657	
Drehersville*	West	0.850	1.30	0.654	
Berwick	North	1.036	1.597	0.649	
Berwick	South	0.960	1.597	0.601	
White Haven	North	1.053	1.636	0.644	
White Haven	South	1.058	1.636	0.647	
Philadelphia**		1.143	1.727	0.622	
Skookumchuck	South	1.126	1.454	0.774	

* Values are based on the AASHO design condition keeping each truck in its respective load lane.

** Without diaphragms.

Table 11. Comparison of Design and Experimental Live Load Moments at the Bridge Midspan

		Design Moment (kip-ft)	Experimental Moment (kip-ft)	Experimental / Design
Exterior Girders				
Dump Truck	Girder A	460.41	563.77	1.224
	Girder E	450.47	500.37	1.111
Tractor Trailer	Girder A	449.67	547.73	1.218
	Girder E	439.95	484.12	1.100
Interior Girders				
Dump Truck	Girder B	588.06	431.07	0.733
	Girder C	588.06	477.21	0.811
	Girder D	588.06	451.57	0.768
Tractor Trailer	Girder B	574.33	430.87	0.750
	Girder C	574.33	476.44	0.830
	Girder D	574.33	430.84	0.750

Table 12. Comparison of the Ratios of Experimental Moment to Design Moment for Drehersville, Berwick, White Haven, Philadelphia and Skookumchuck.

	$\frac{\text{Experimental Moment}}{\text{Design Moment}}$	
	Interior Girders	Exterior Girders
Drehersville	0.667	1.416
Berwick	0.648	1.121
White Haven	0.643	1.187
Philadelphia	0.663	1.108
Skookumchuck	0.742 (Girder B)	1.221 (Girder A)
	0.820 (Girder C)	1.105 (Girder E)
	0.759 (Girder D)	

Table 13. Tabulation of Maximum Strains (10^{-6} in/in) on Bottom Surfaces of Girders for White Haven, Berwick and Skookumchuck Bridges.

Truck Location	Girder A		Girder B	
	Left	Right	Left	Right
		White Haven		
Lane 1	51.6	59.2	48.6	41.8
2	37.1	38.5	49.5	45.8
3	24.9	23.9	40.2	42.1
4	17.0	13.8	30.1	28.3
5	10.6	8.3	23.0	19.2
Lanes 1 and 4 (superimposed)	68.6	73.0	78.7	70.1
		Berwick		
Lane 1	38.9	42.0	34.8	30.9
2	31.4	30.1	34.0	34.2
3	23.2	19.5	29.5	32.2
4	17.9	15.0	23.6	23.7
5	11.7	9.2	18.9	15.8
Lanes 1 and 4 (superimposed)	56.8	57.0	58.4	54.6
		Skookumchuck		
Lane 5	26.38	26.31	20.08	17.37
4	18.57	19.59	21.53	21.93
3	4.26	5.92	13.25	13.03
2	3.59	3.22	5.59	5.00
1	3.38	3.22	4.35	3.91
Lanes 1, 3 and 5 (superimposed)	34.02	35.45	37.68	34.31

Table 14. Moment Percentage at the Bridge Midspan as Calculated by Finite Element Theory, and The Theoretical Design Factors.

$$\text{MOMENT PERCENTAGE} = \frac{\text{MOMENT}}{\Sigma\,\text{MOMENT}}\ (100)$$

	DUMP TRUCK GIRDER					TRACTOR TRAILER GIRDER				
	A	B	C	D	E	A	B	C	D	E
Lane 1	6.54	8.16	14.08	28.90	42.32	7.36	8.84	15.07	27.86	40.87
Lane 3	15.22	19.91	30.32	19.83	14.72	16.23	20.25	27.40	20.07	16.05
Lane 5	42.20	28.90	14.00	8.07	6.63	41.08	27.88	15.03	8.79	7.22
Design Factor	1.283	1.139	1.168	1.136	1.273	1.293	1.139	1.150	1.134	1.283
Theoretical Design	1.127	0.783	0.803	0.781	1.143	1.136	0.783	0.791	0.780	1.152

11. FIGURES

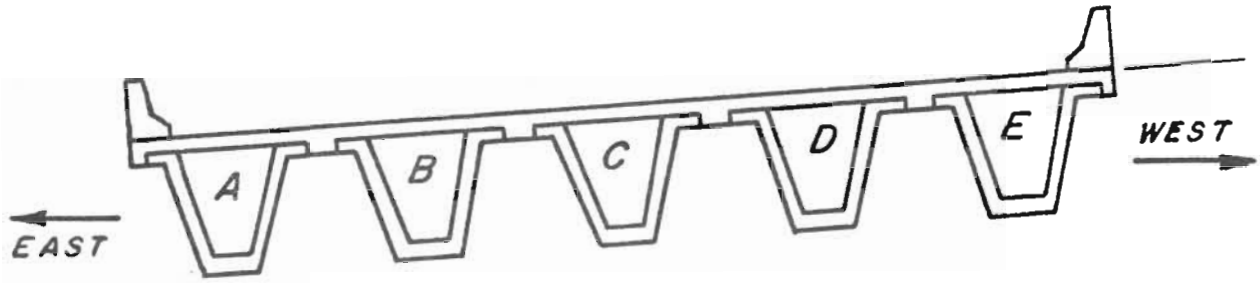

TYPICAL CROSS SECTION SHOWING
GIRDER IDENTIFICATION AND
SUPERELEVATION.

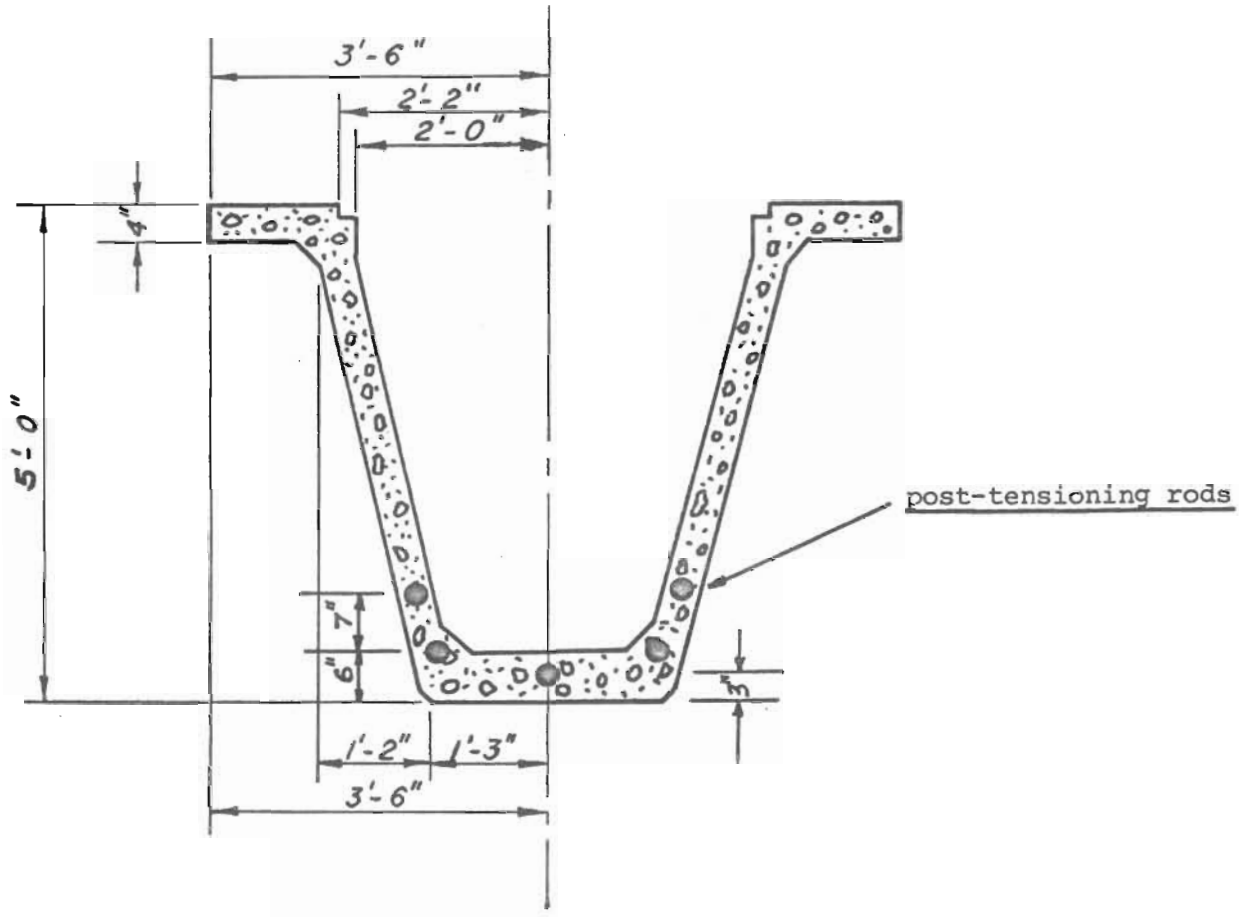

TYPICAL SECTION (MID SPAN)

Figure 2. Typical Cross Section and U-Shaped Girder Detail at Mid Span.

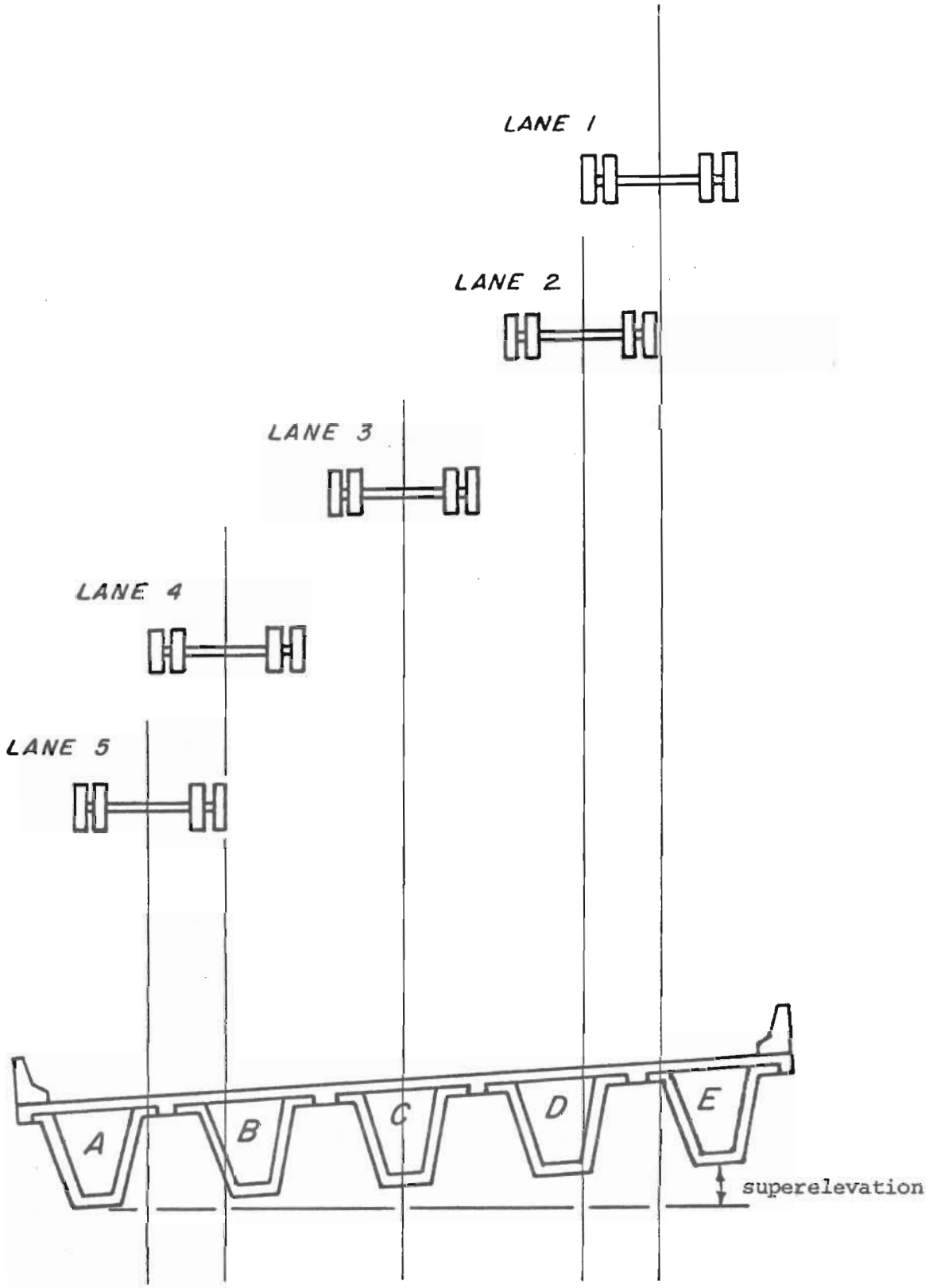

Figure 3. Experimental Loading Lanes. Loading Lanes 1, 3 and 5 are those used in the Theoretical Analysis.

Figure 4. Skookumchuck Creek Bridge.

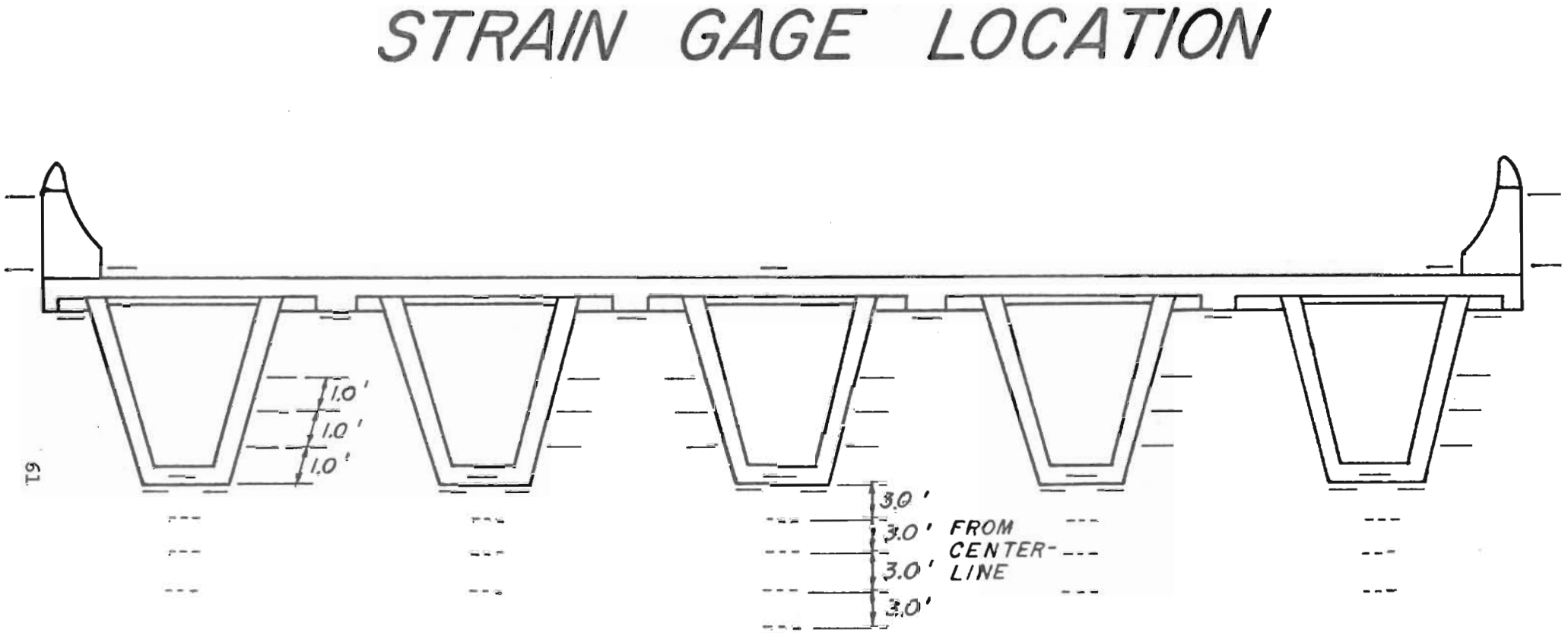

Figure 5. Strain Gage Location.

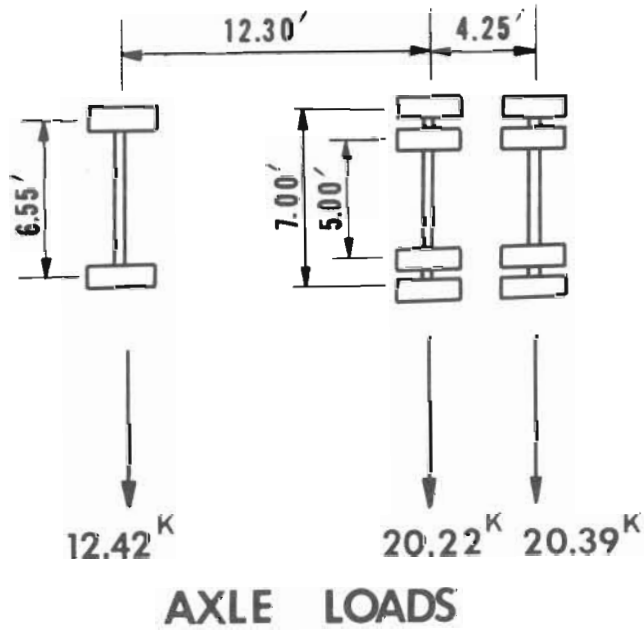

Figure 6. Dump Truck.

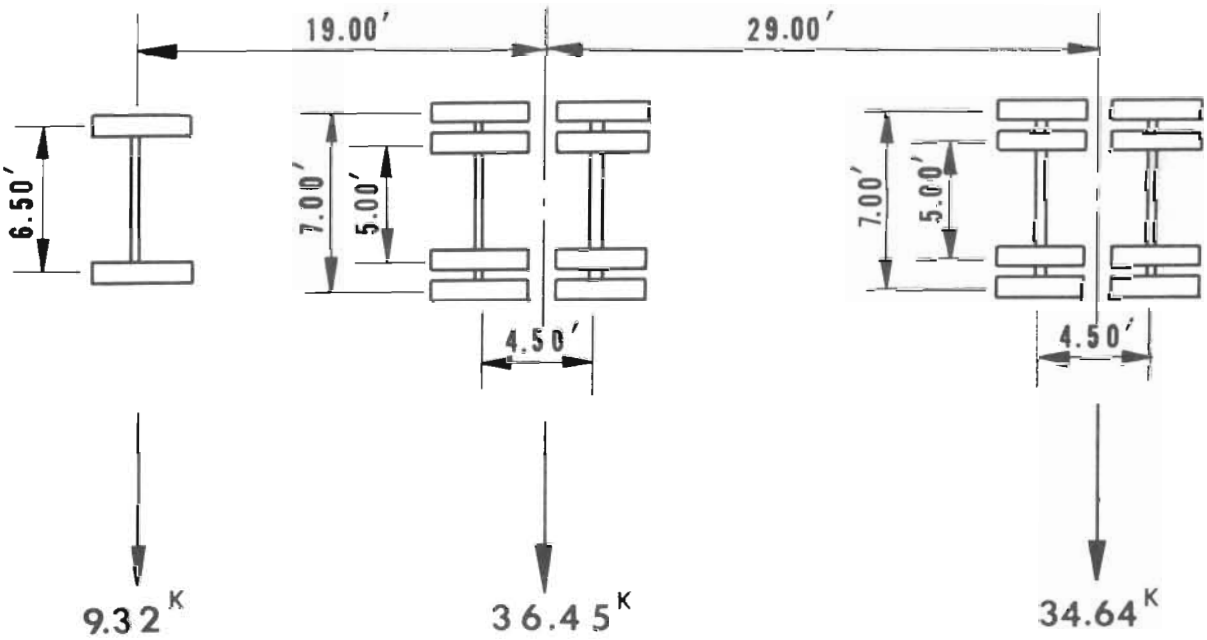

Figure 7. Tractor Trailer.

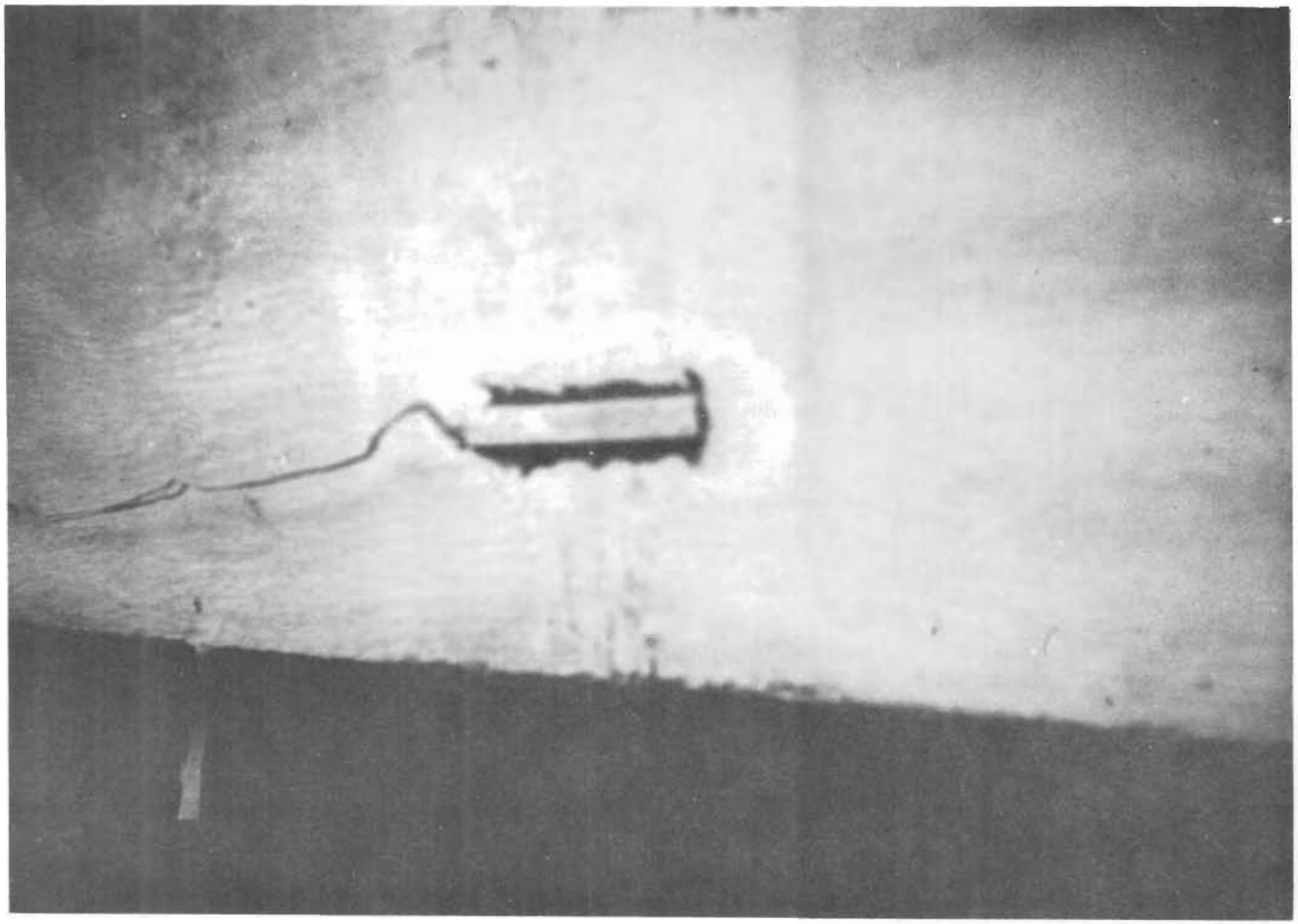

Figure 8. Photograph of a Strain Gage in Place. (PML-60).

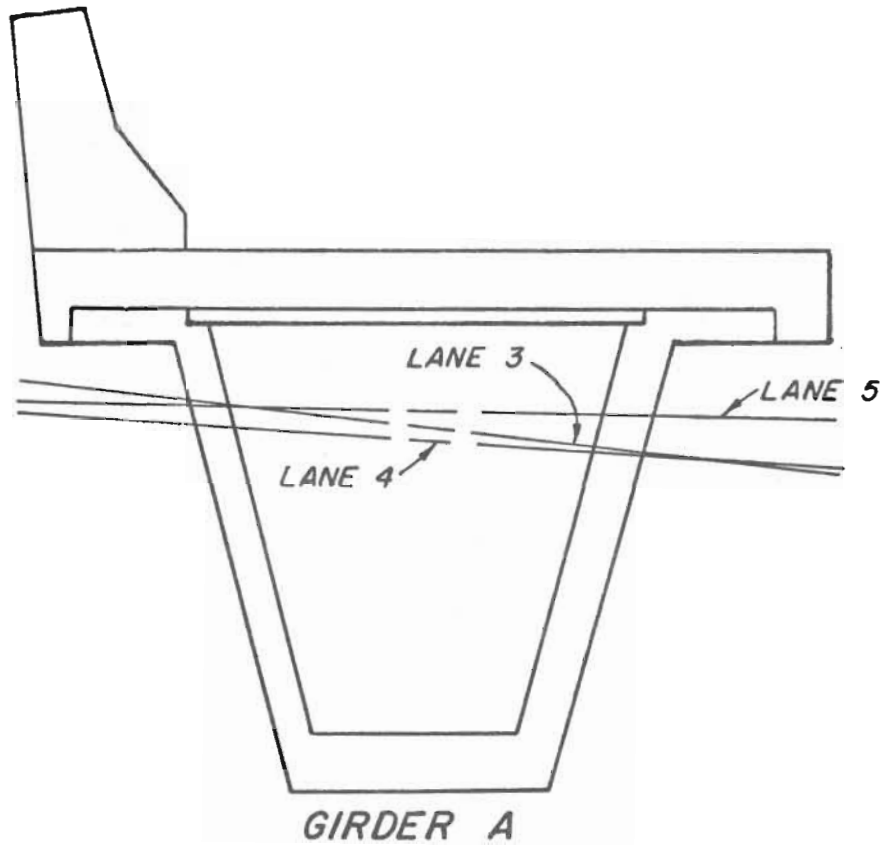

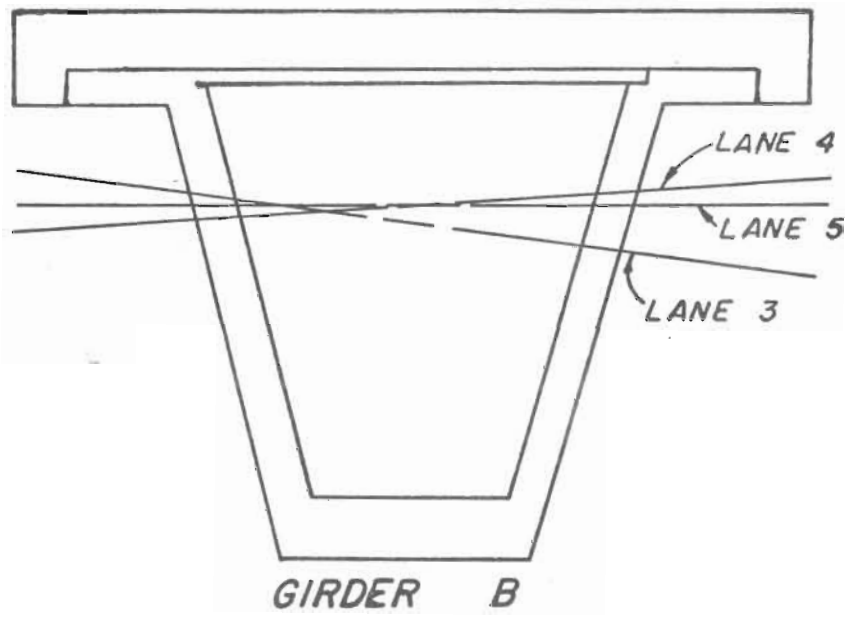

Figure 9. Typical Examples of Experimental Neutral Axis Location for the Tractor Trailer.

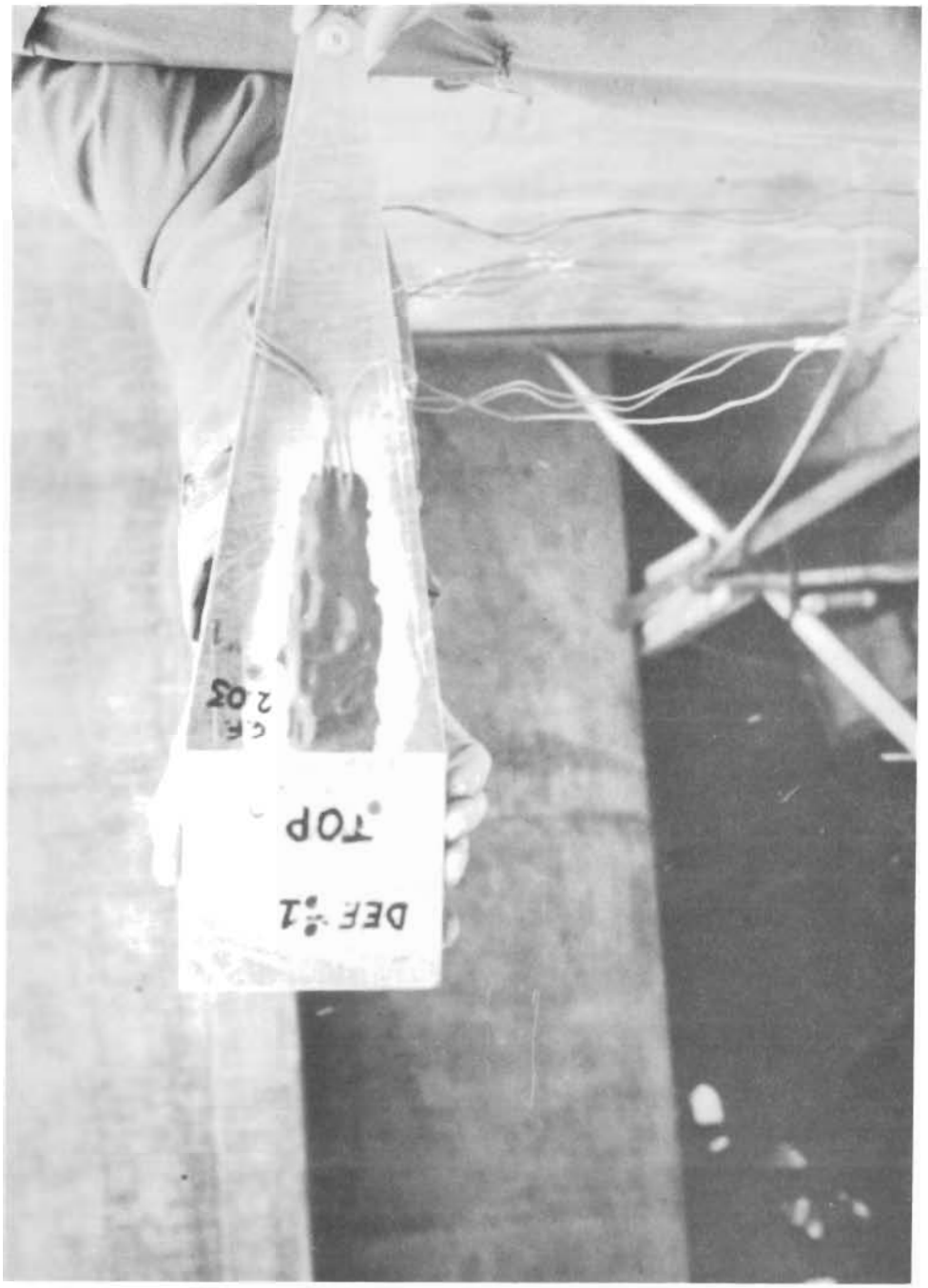

Figure 10. Cantilevered Beam Deflectometer.

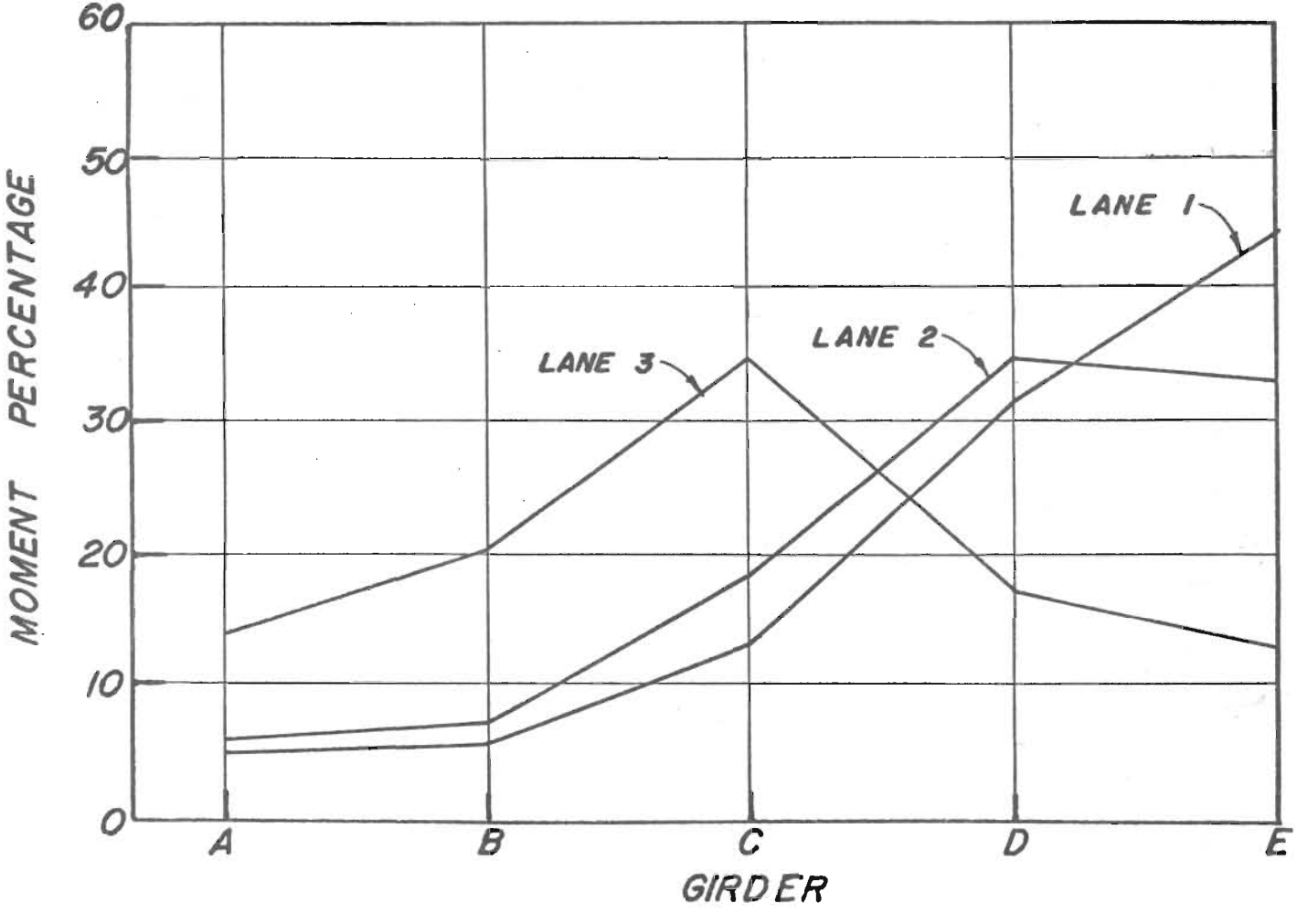

Figure 11. Moment Percentage at the Bridge Midspan for the Dump Truck. Lanes 1, 2 and 3.

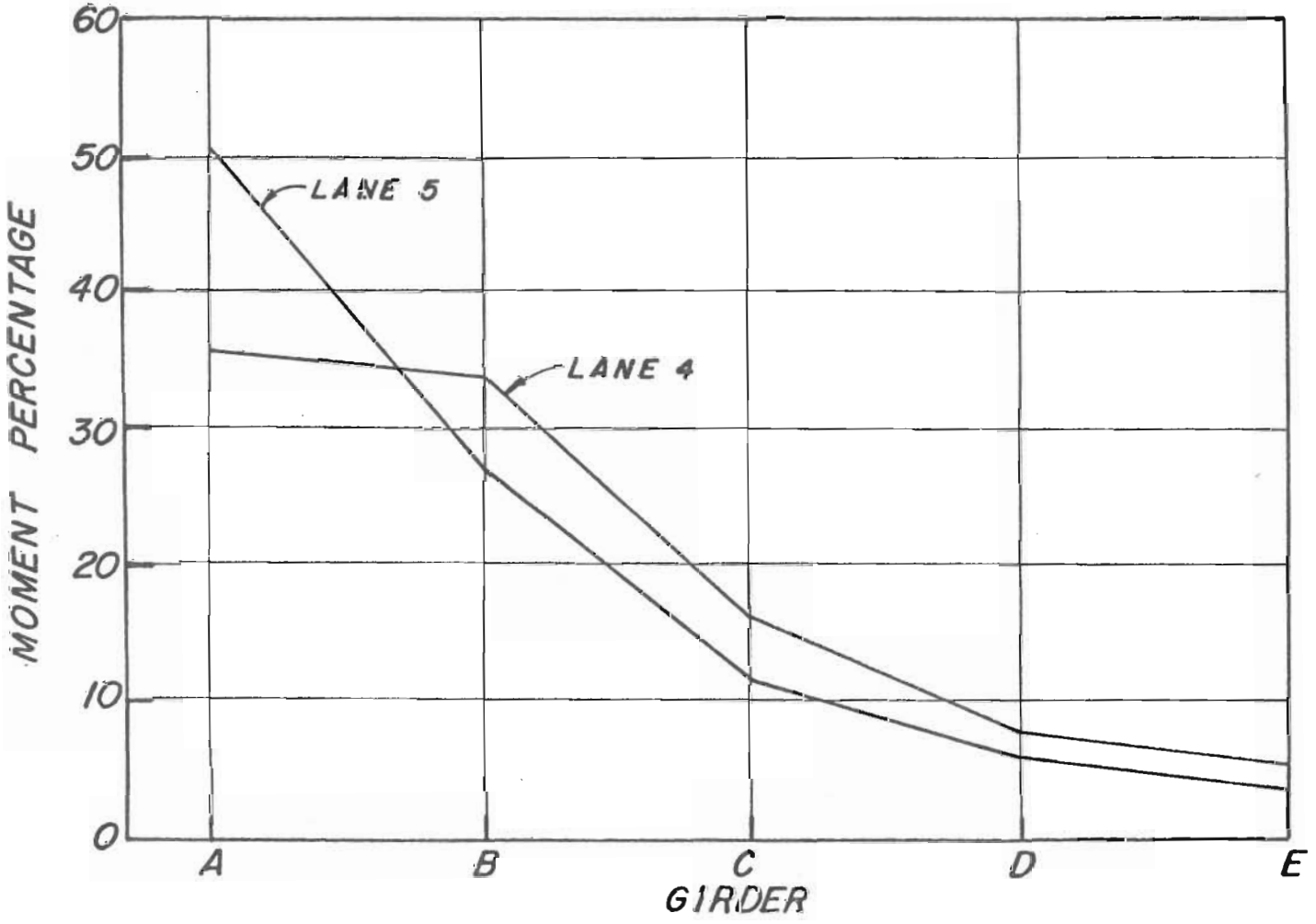

Figure 12. Moment Percentage at the Bridge Midspan for the Dump Truck. Lanes 4 and 5.

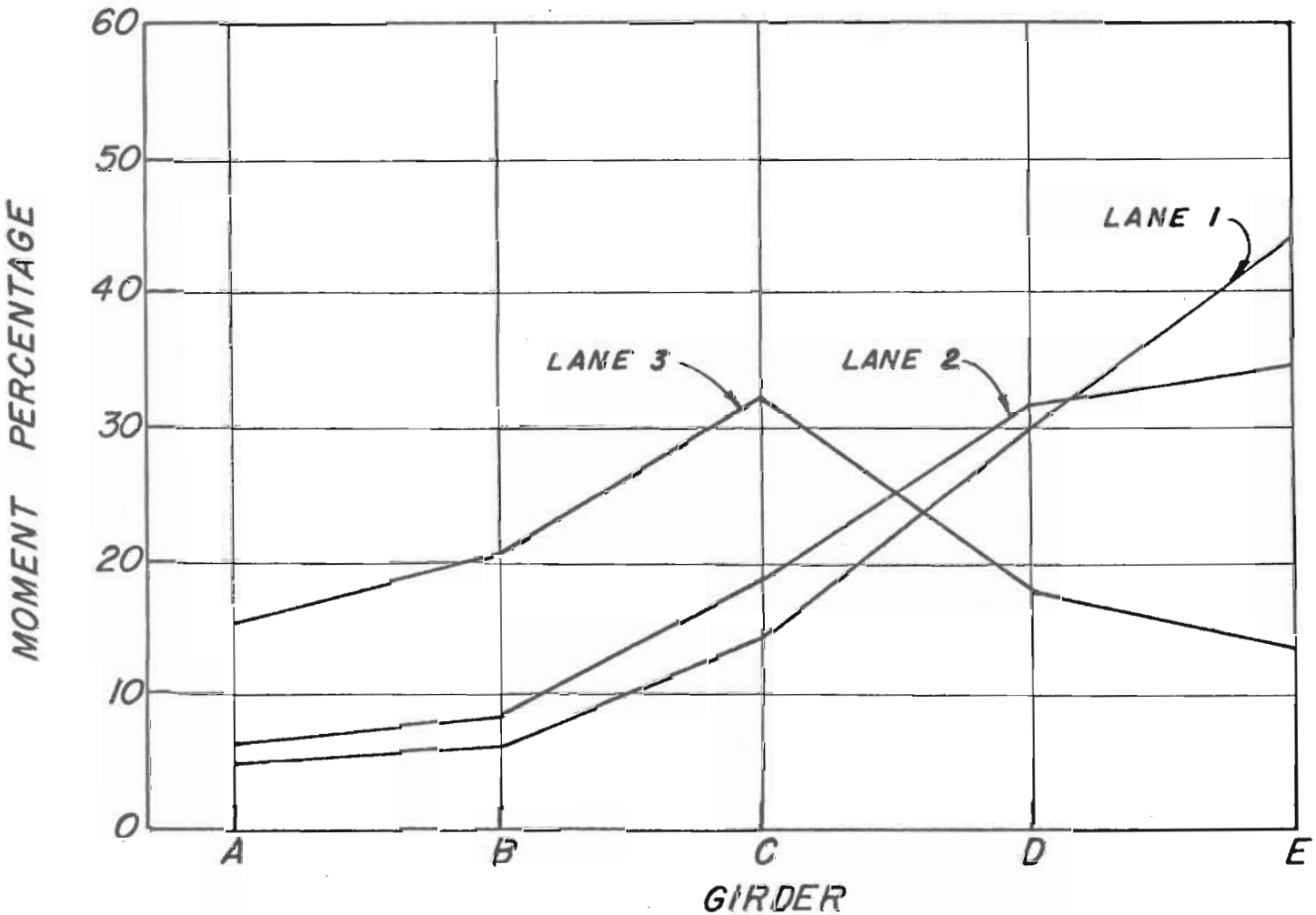

Figure 13. Moment Percentage at the Bridge Midspan for the Tractor Trailer. Lanes 1, 2 and 3.

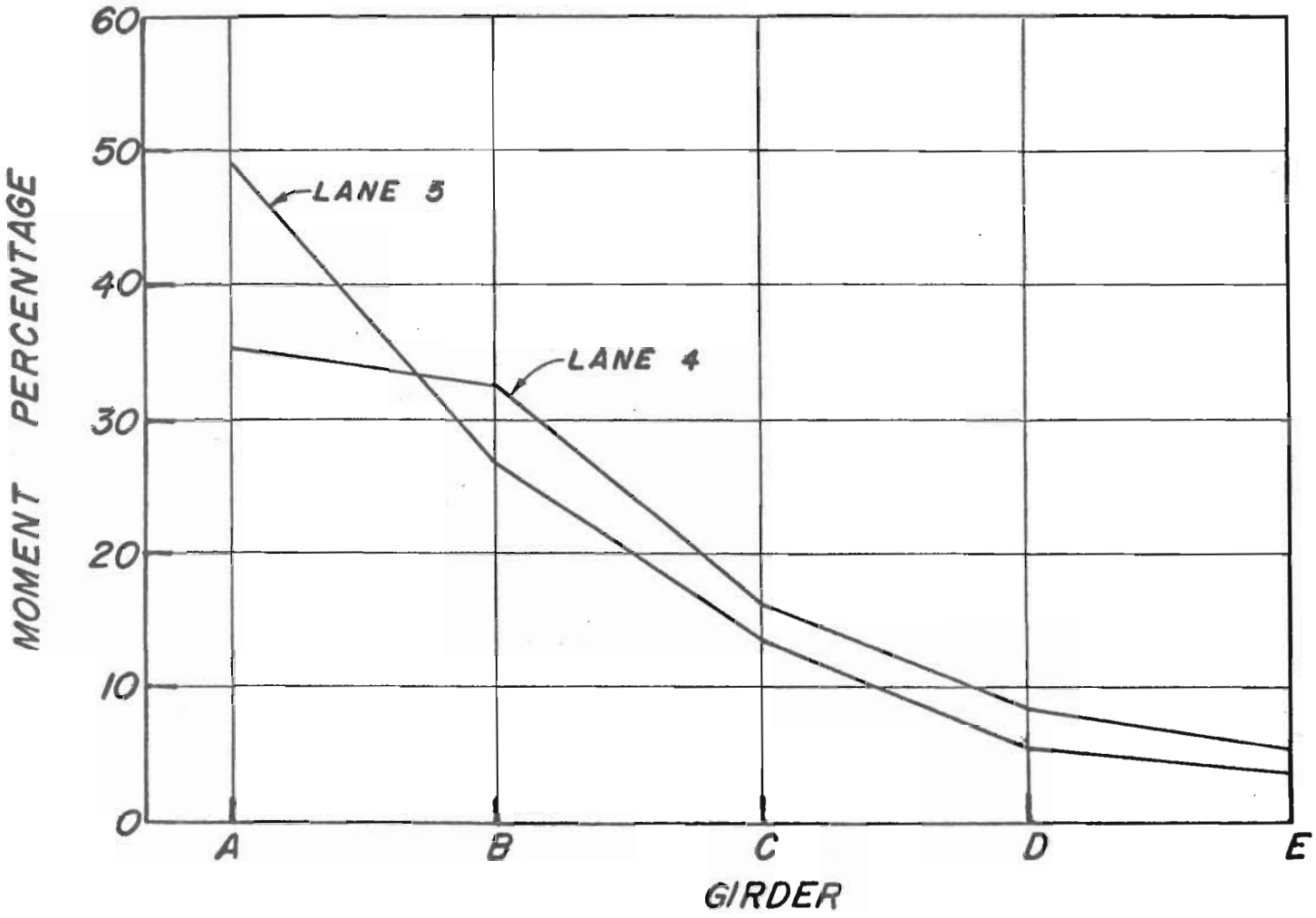

Figure 14. Moment Percentage at the Bridge Midspan for the Tractor Trailer. Lanes 4 and 5.

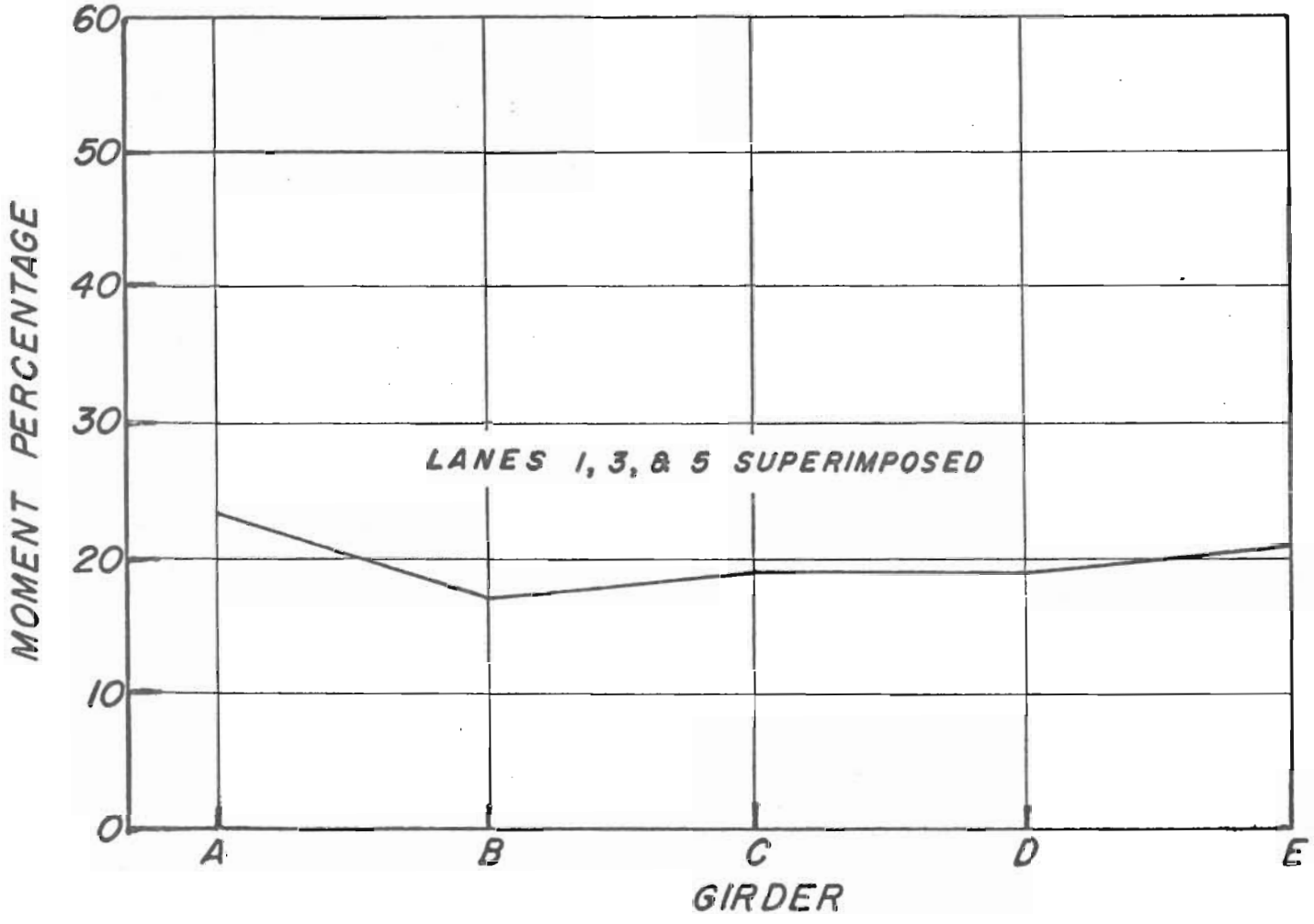

Figure 15. Moment Percentage at the Bridge Midspan for the Dump Truck. Lanes 1, 3 and 5 superimposed.

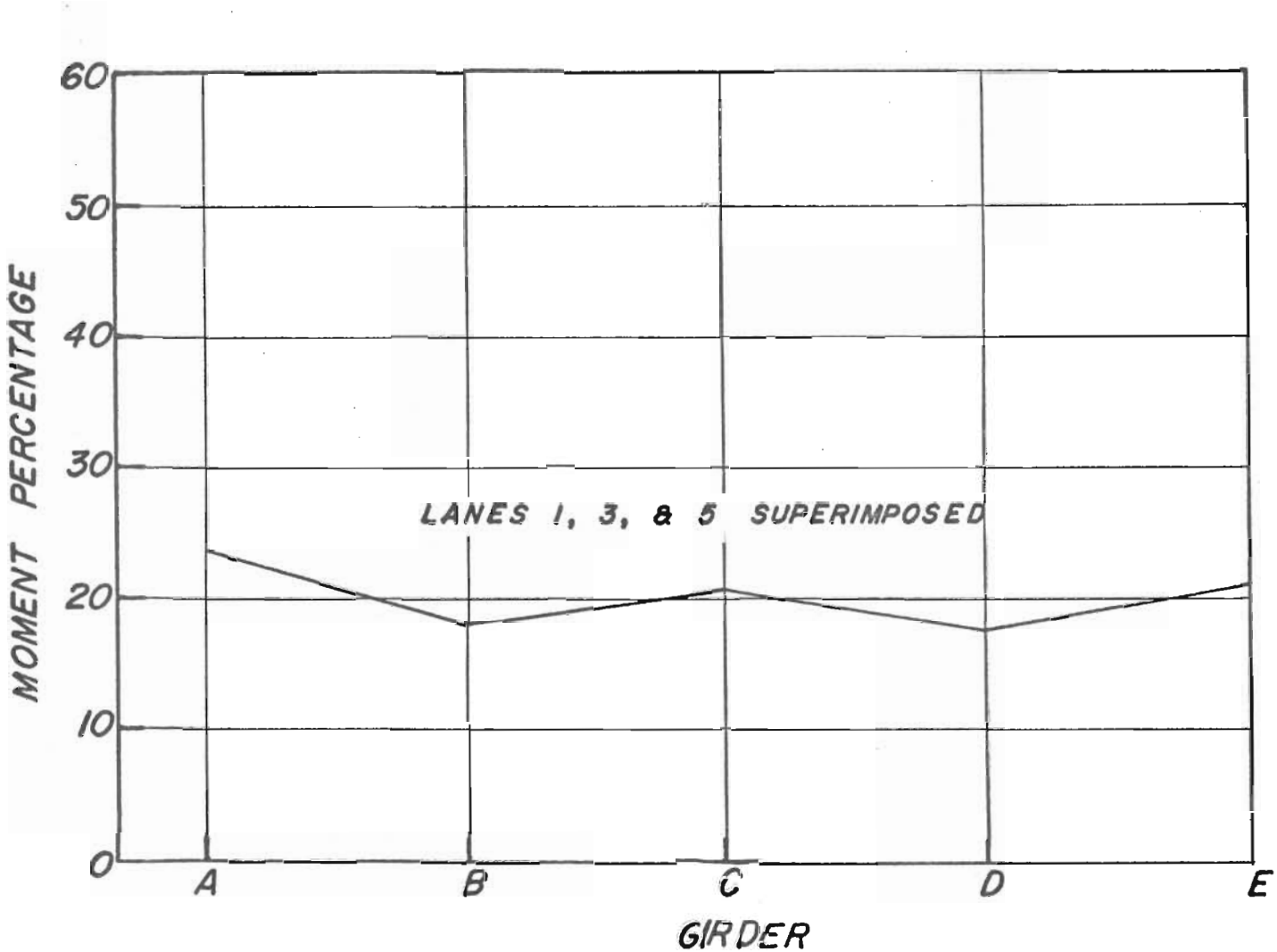

Figure 16. Moment Percentage at the Bridge Midspan for the Tractor Trailer. Lanes 1, 3 and 5 superimposed.

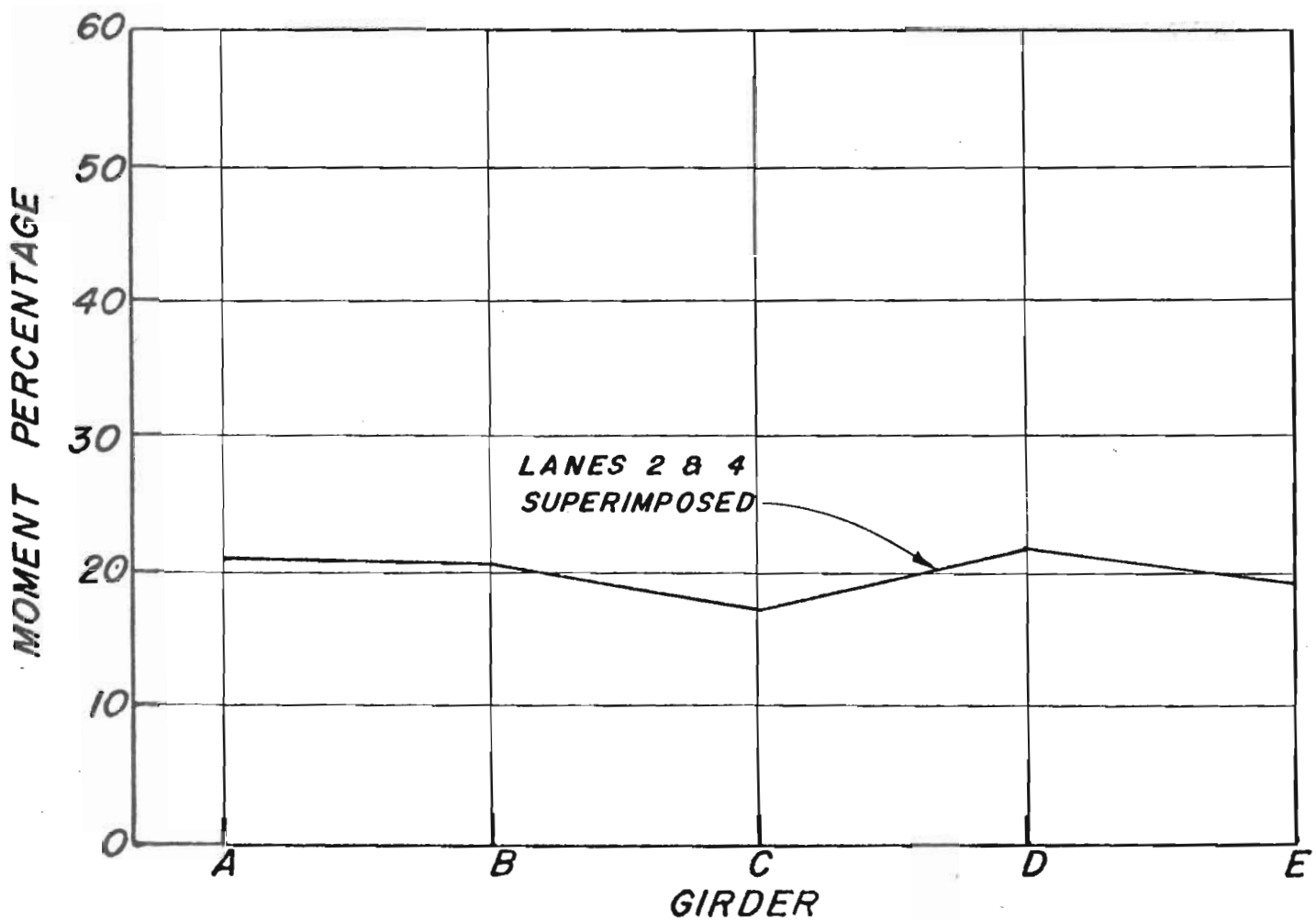

Figure 17. Moment Percentage at the Bridge Midspan for the Dump Truck. Lanes 2 and 4 superimposed.

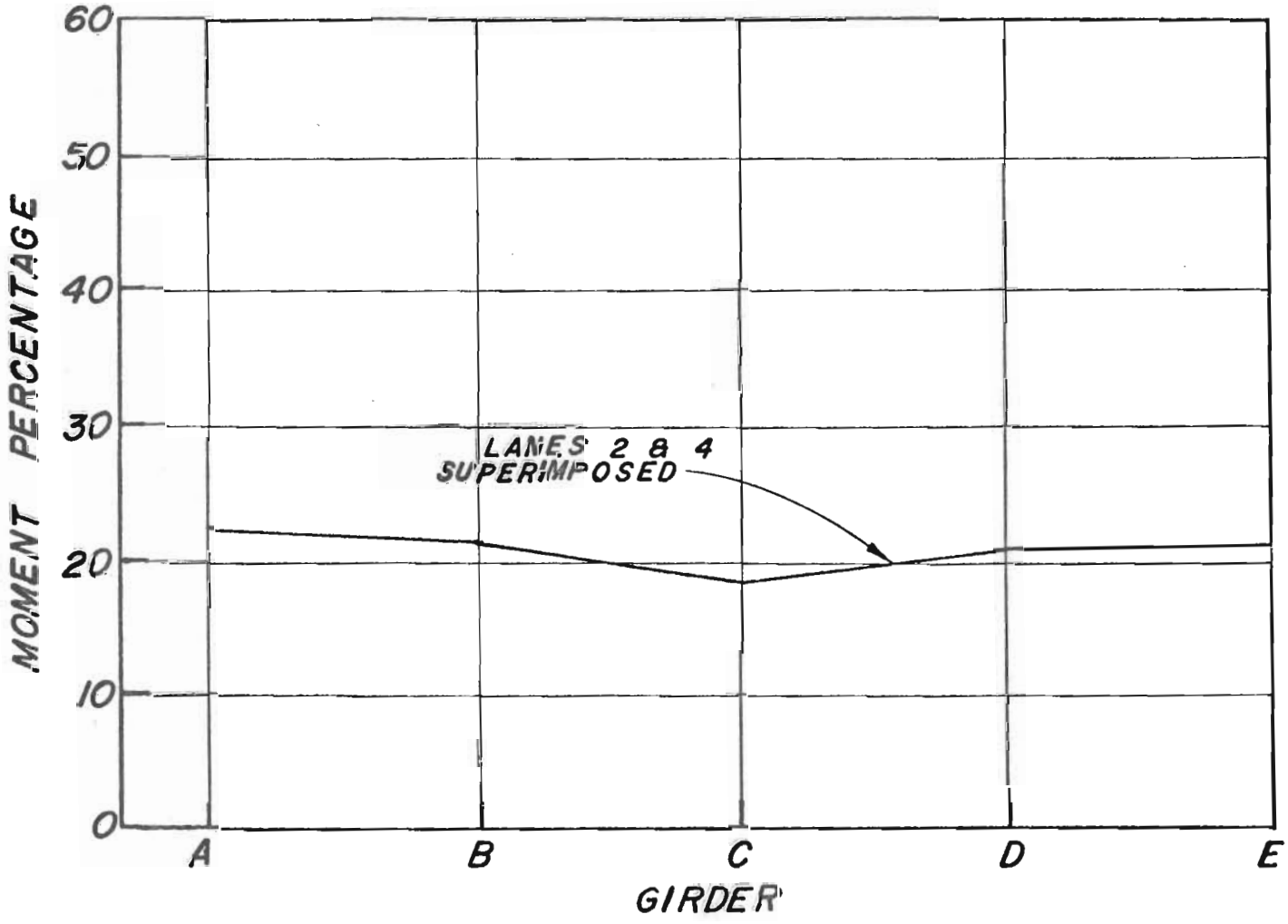

Figure 18. Moment Percentage at the Bridge Midspan for the Tractor Trailer. Lanes 2 and 4 superimposed.

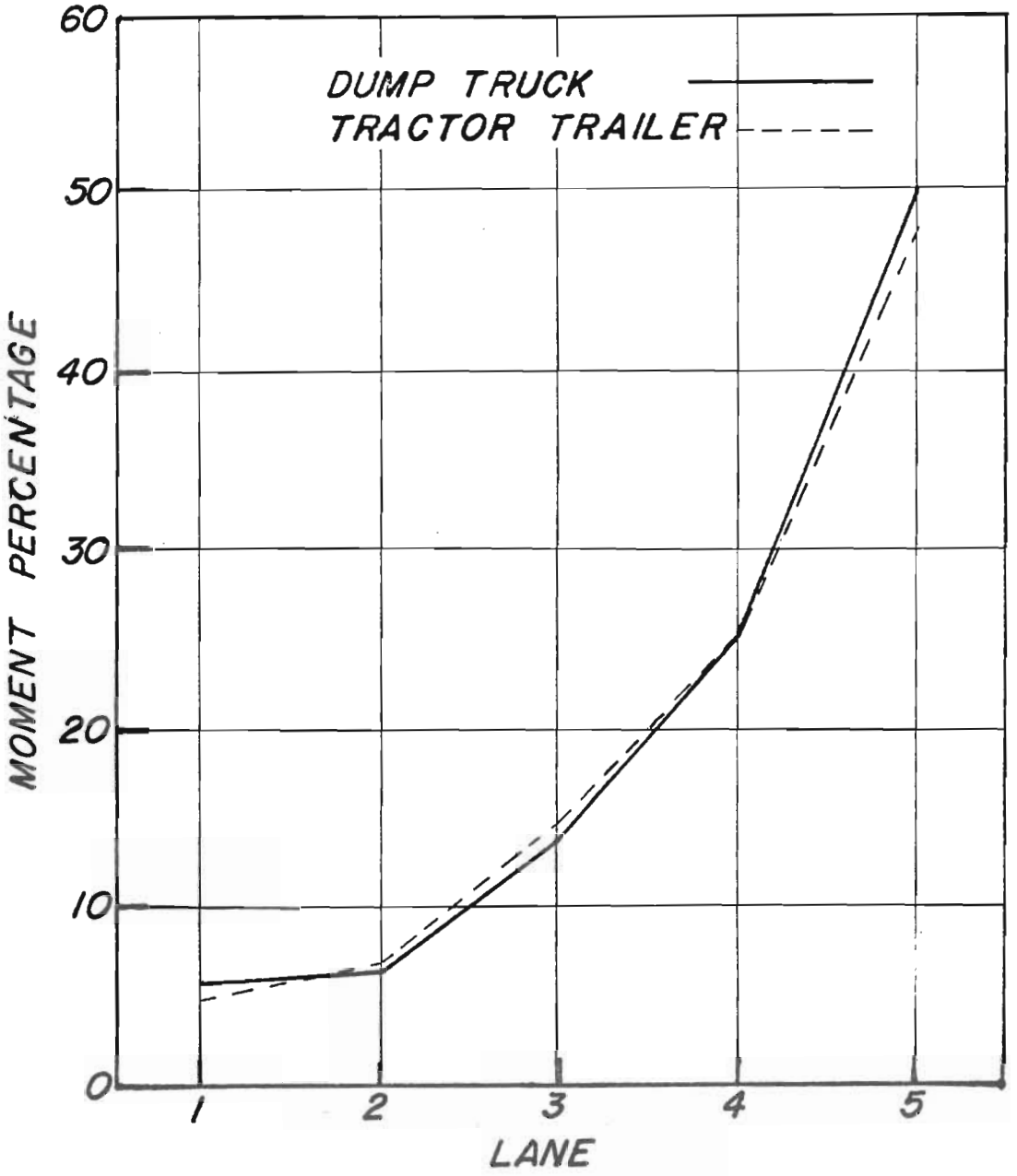

Figure 19. Influence Line for Beam A.

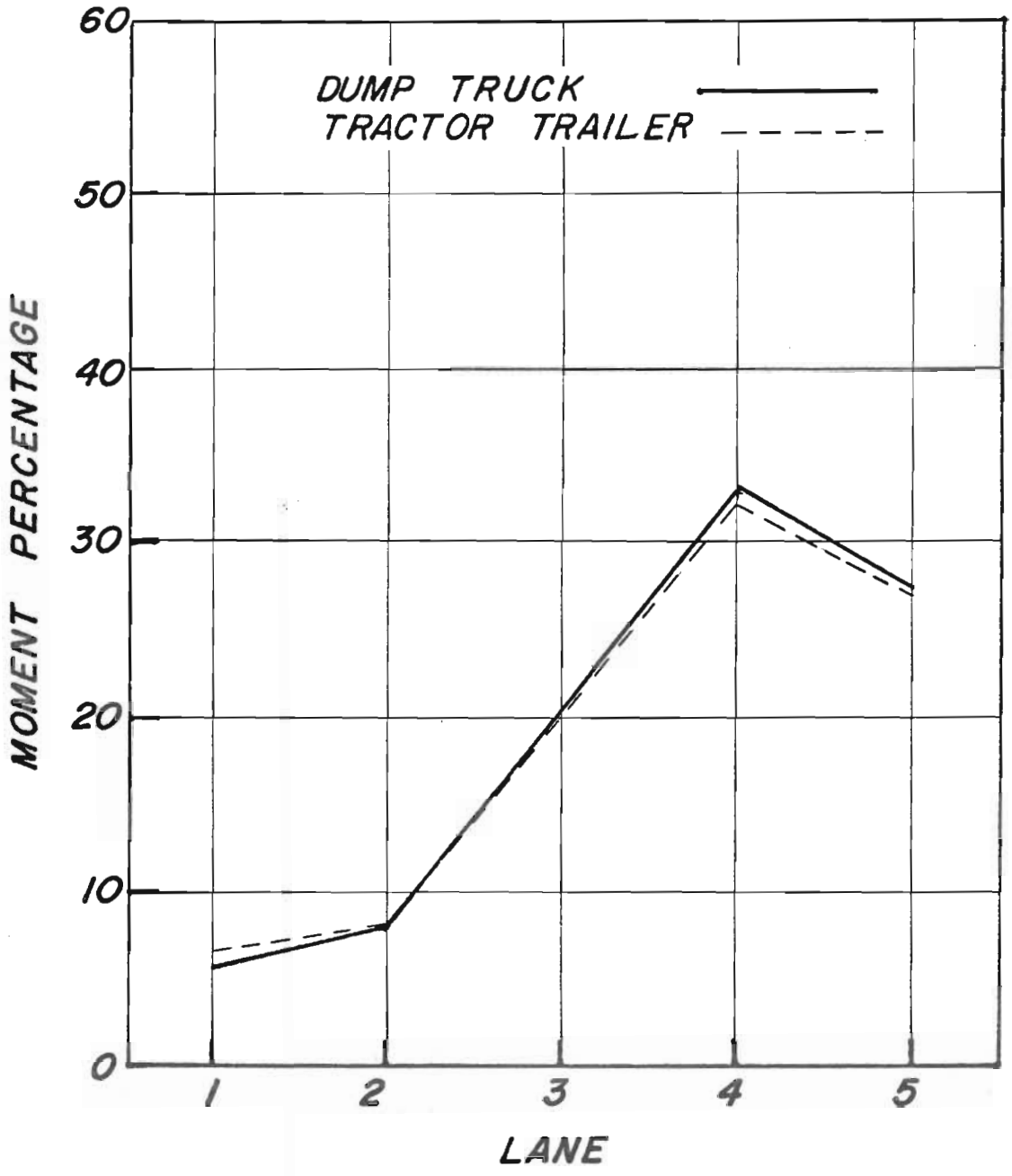

Figure 20. Influence Line for Beam B.

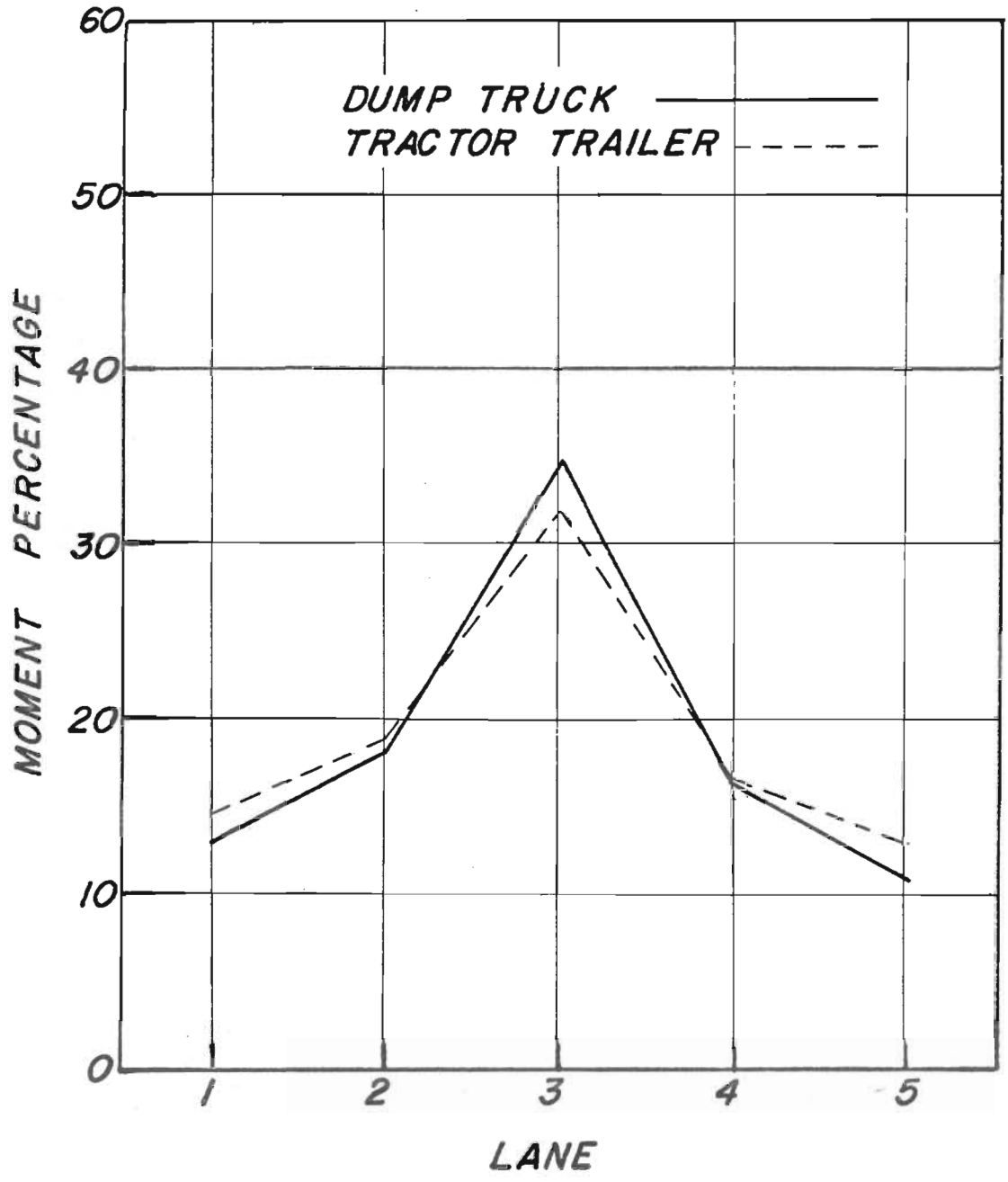

Figure 21. Influence Line for Beam C.

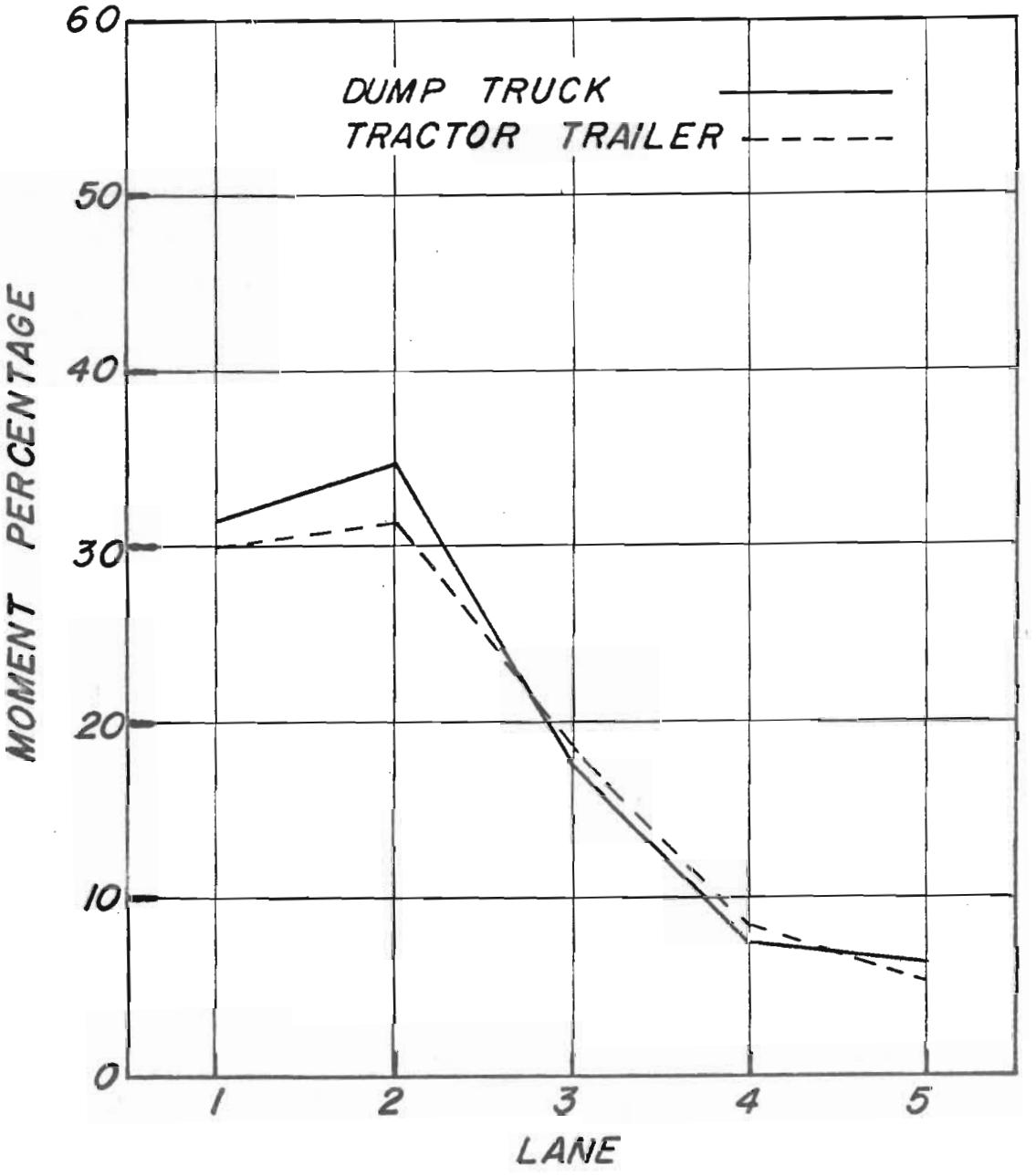

Figure 22. Influence Line for Beam D.

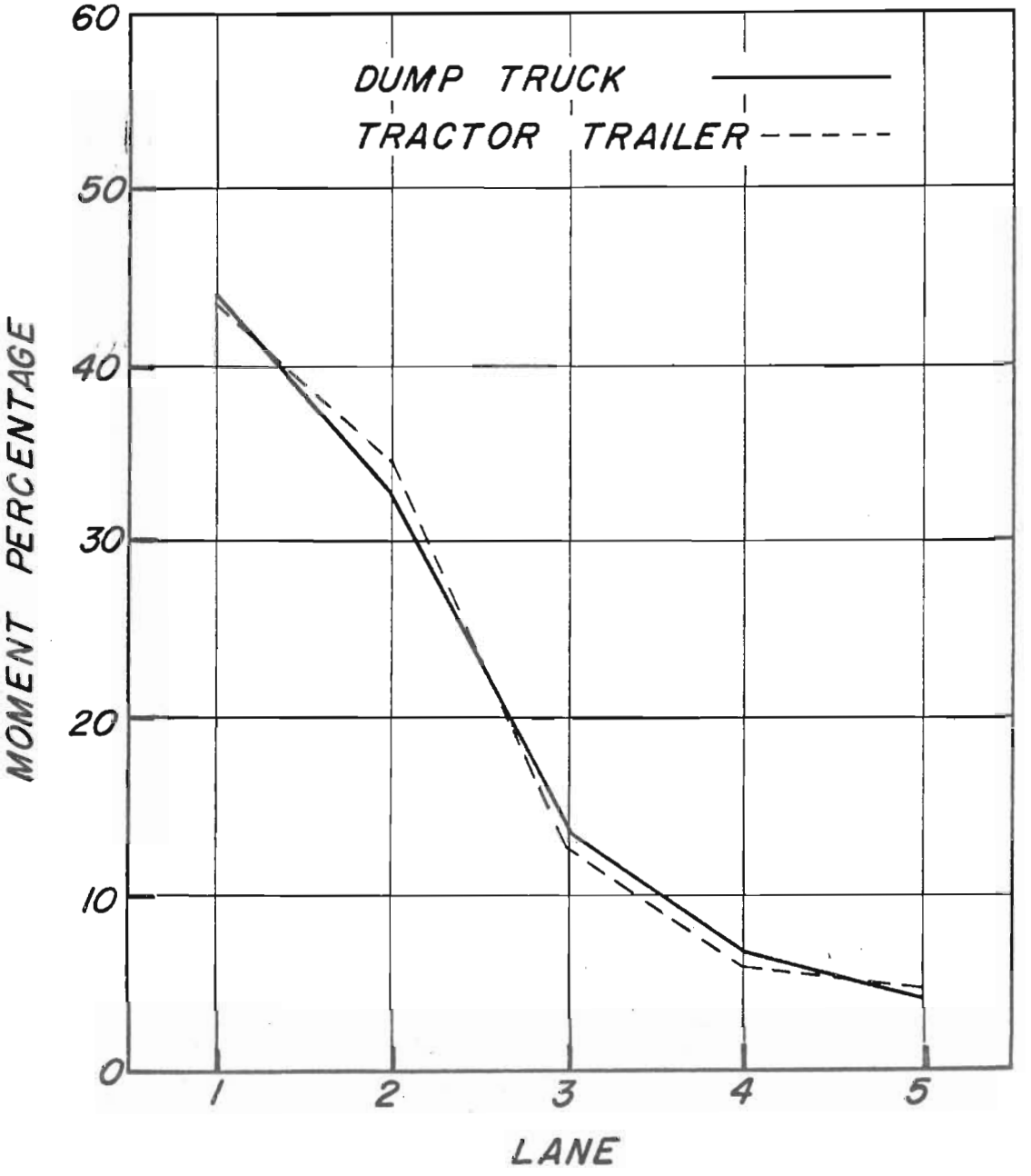

Figure 23. Influence Line for Beam E.

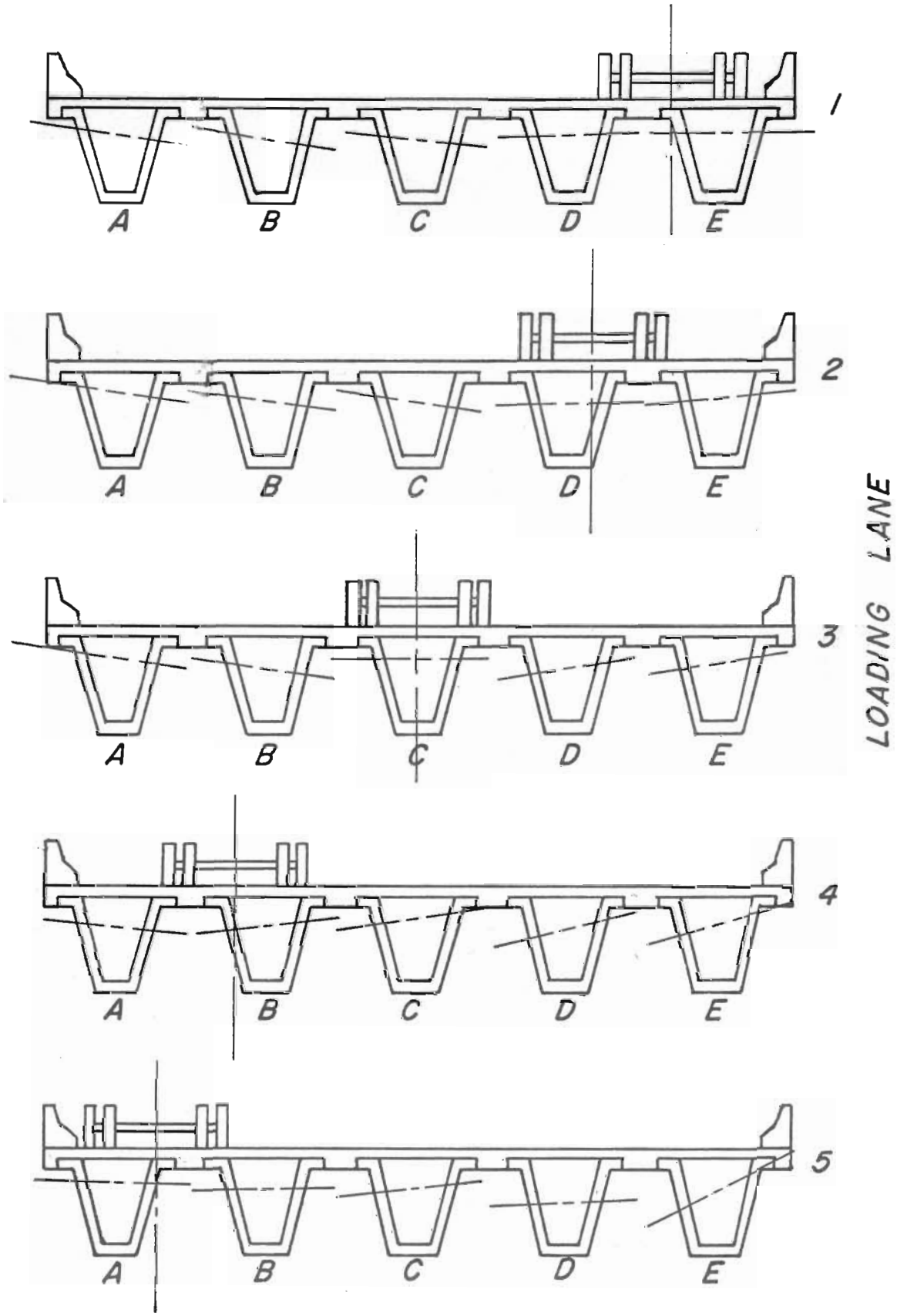

Figure 24. Experimental Neutral Axis Location. Results for the Tractor Trailer.

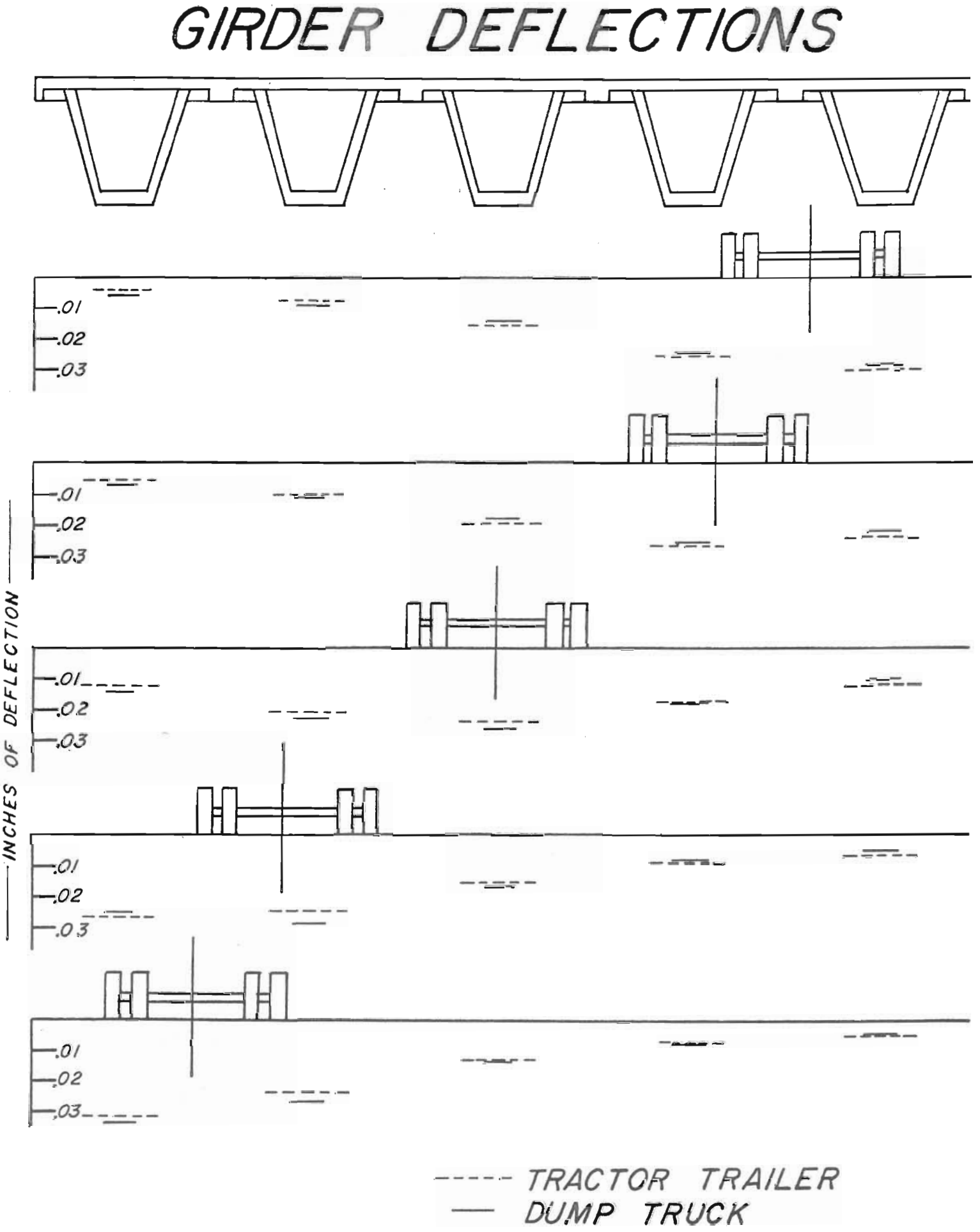

Figure 25. Girder Deflections.

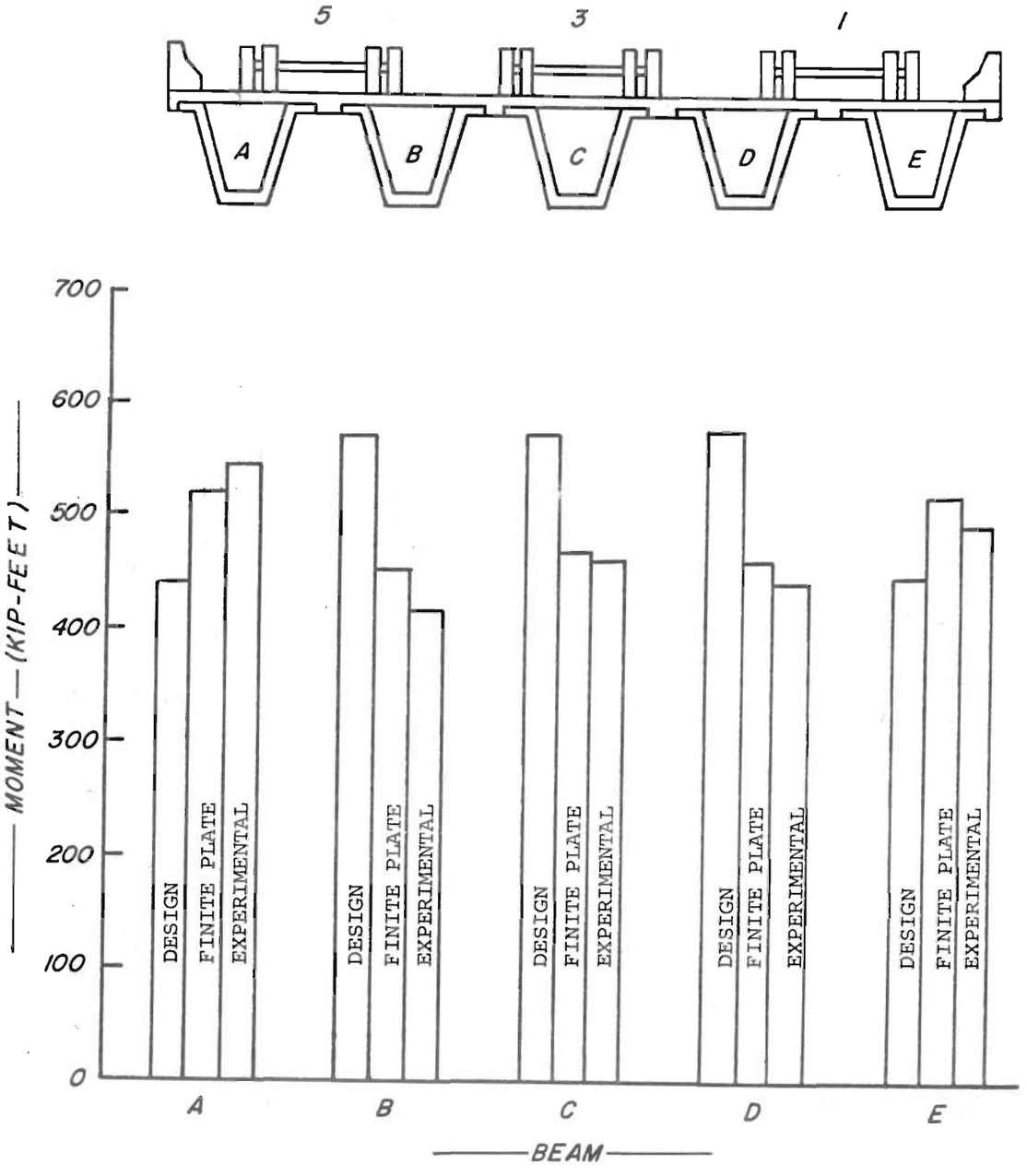

Figure 26. Design, Theoretical and Experimental Live Load Moments for the Dump Truck.

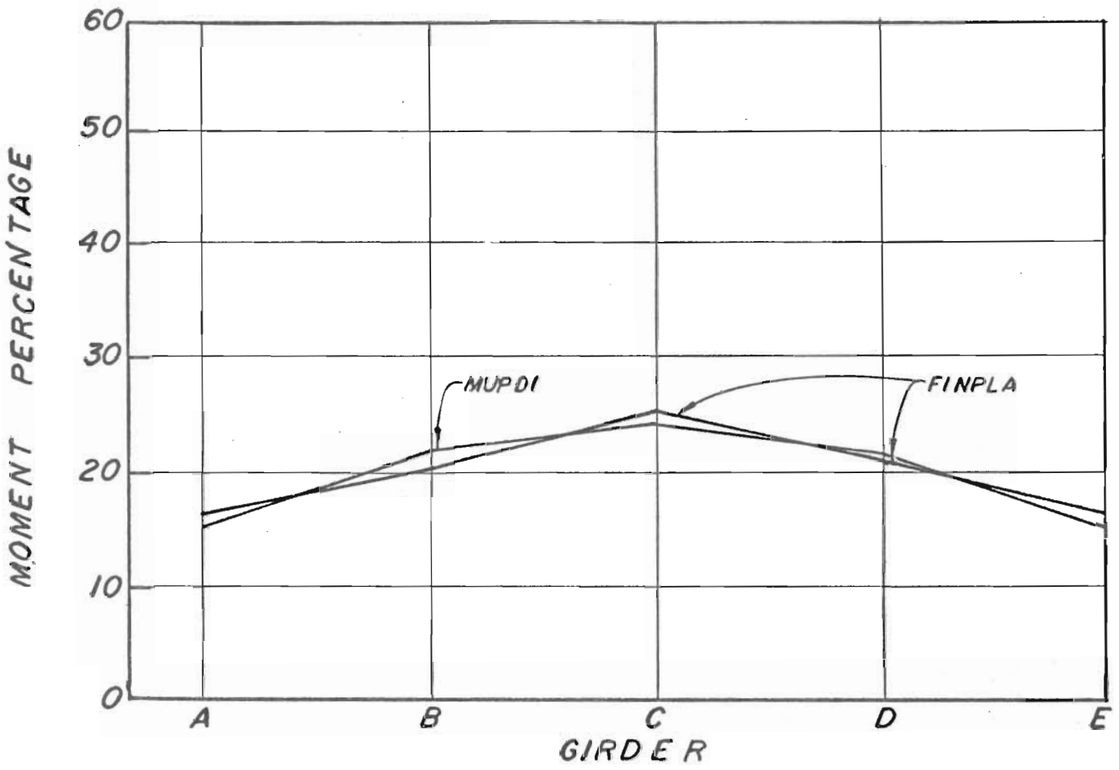

Figure 28. A Comparison of Moment percentages at the Bridge Midspan for a Modified HS 20-44 Truck in Loading Lane 3 as Calculated by Folded Plate (MUPDI) and Finite Element (FINPLA) Theory.

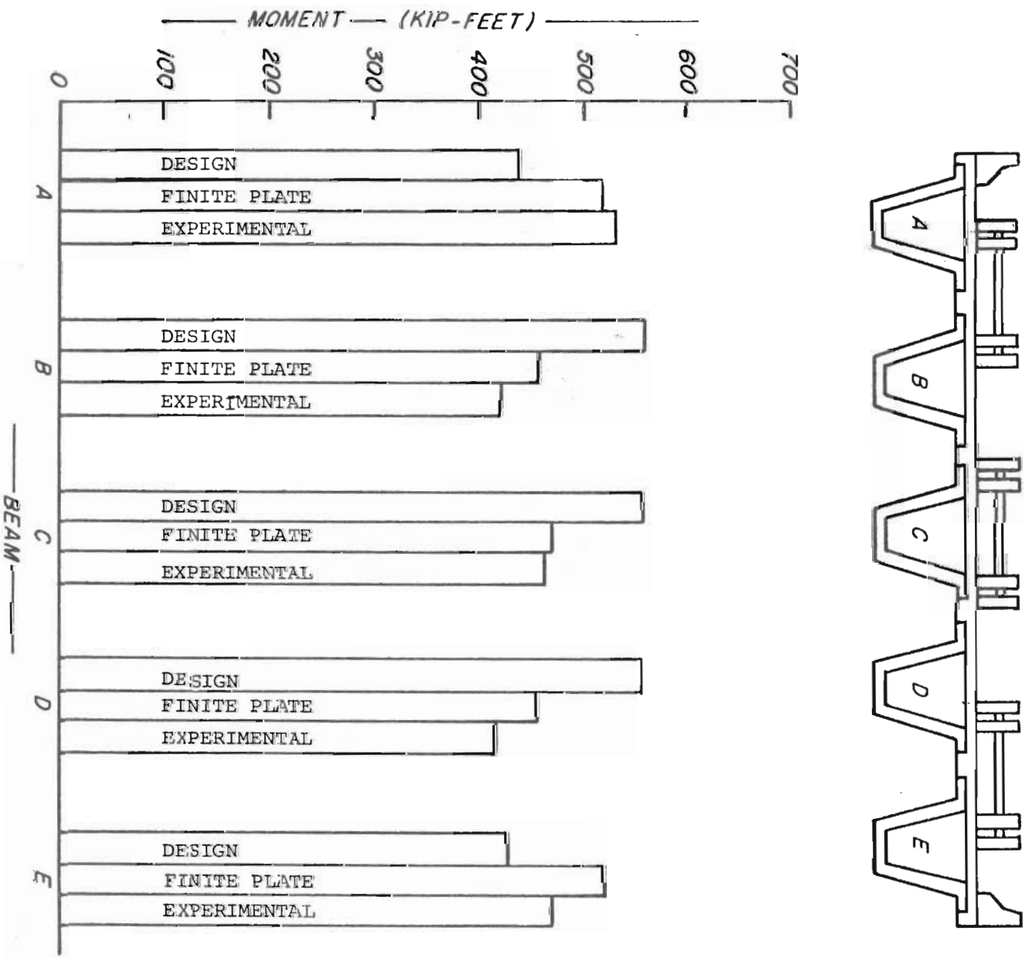

Figure 27. Design, Theoretical and Experimental Live Load Moments for the Tractor Trailer.

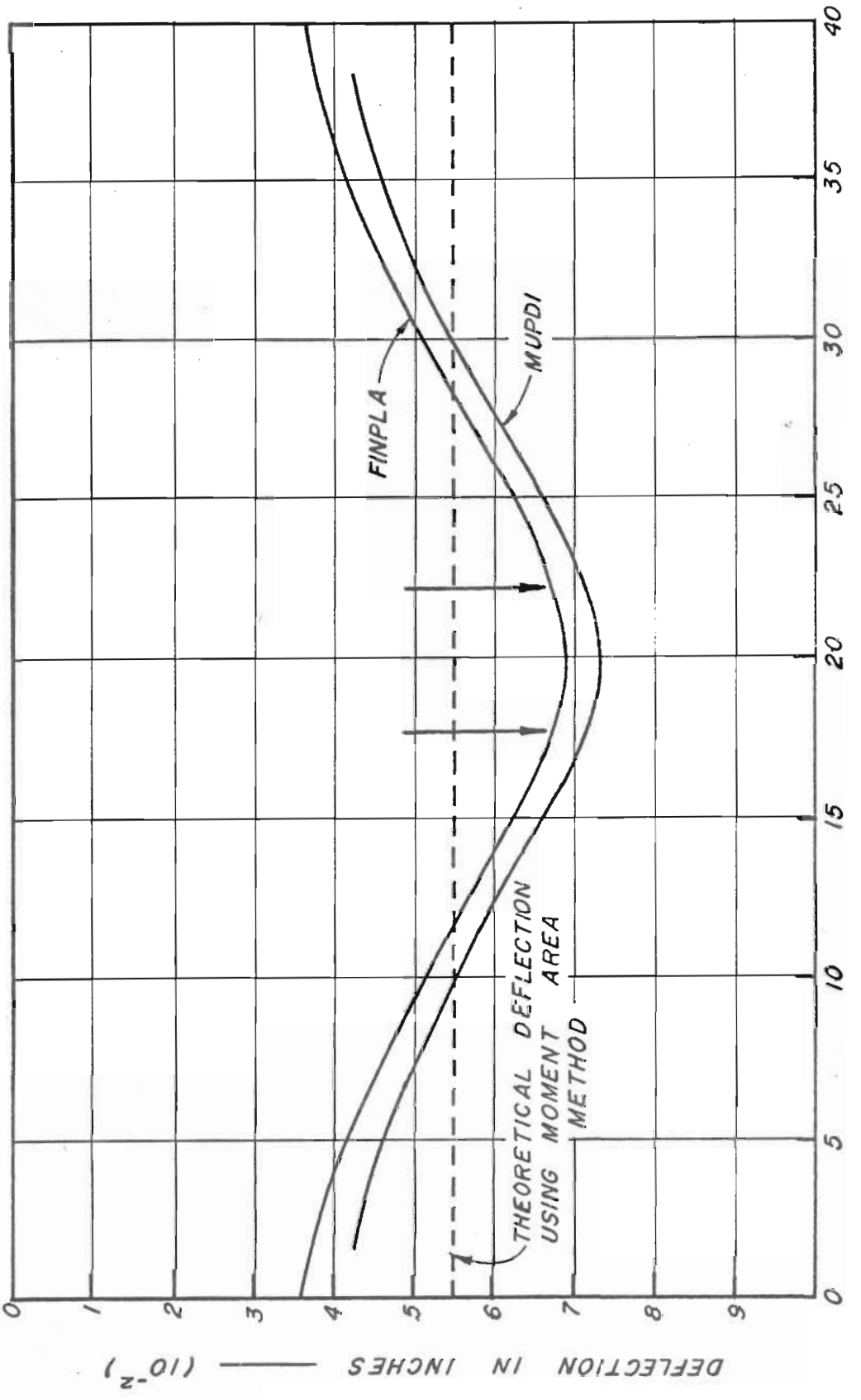

Figure 29. Transverse Variation of Midspan Deflection for the modified HS 20-44 Truck.